Annu. Rev. Astron. Astrophys. 1995. 33:239–82

HIGH-ENERGY PARTICLES IN SOLAR FLARES

H. Hudson

Institute for Astronomy, University of Hawaii, 2680 Woodlawn Drive, Honolulu, Hawaii 96822

J. Ryan

Space Science Center, University of New Hampshire, Durham, New Hampshire 03824-3525

KEY WORDS: Sun, particle acceleration, X rays, γ rays, *Compton Gamma Ray Observatory, Yohkoh*

ABSTRACT

Accelerated particles appear to coexist inseparably with most forms of energy release in solar flares and coronal mass ejections. We identify at least five different populations of high-energy electrons and ions. High-energy particles, accelerated efficiently in the flare in great numbers, transport a large fraction of the flare energy to other sites. This behavior makes them an integral part of the flare process. Much new data has come from two spacecraft launched in 1991: the *Compton Gamma-Ray Observatory* and *Yohkoh*. This review concentrates on particles in flares, mainly using X-ray and gamma-ray data rather than measurements of "escaping" particles observed in interplanetary space.

1. INTRODUCTION

We find evidence for nonthermal particle acceleration in almost all forms of solar magnetic activity and we further conclude that the role of the accelerated particles is significant for an understanding of the physics. We review here what we have learned recently about these energetic particles from hard X-ray data and γ-ray data, with emphasis on remote-sensing measurements of the particles in the solar active plasmas themselves, rather than on in situ measurements in the interplanetary medium.

0066-4146/95/0915-0239$05.00

Two new spacecraft launched in 1991, the *Compton Gamma Ray Observatory* (*CGRO*) and *Yohkoh*, instrumented to measure γ rays and X rays, respectively, provide the bulk of the material for this review. Each of these spacecraft has improved tremendously the capability for solar high-energy observations. Their new results have provided some clarification of known effects and some surprises. Significant contributions to understanding solar energetic particles have also come from the *GRANAT* and *GAMMA-1* spacecraft as well as from ground-based observatories.

The solar cycle determines the occurrence rate of solar flares, so if we assume that the solar maximum occurred at 1991.0, then the literature cutoff date for this review falls approximately at phase $2\pi/3$ out of a 10.6-year half-cycle—sufficient to have gleaned the main results from the major flares of this cycle. However, the new instrumentation has much greater sensitivity and dynamic range than that of previous generations, so that interesting results from minor nonthermal activity (microflares, X-ray jets, etc) continue to appear.

Related reviews in the past decade in this journal include "Solar Flares and Coronal Mass Ejections" (Kahler 1992), "Flares on the Sun and Other Stars" (Haisch et al 1991), "Classification of Solar Flares" (Bai & Sturrock 1989), "Radio Emission from the Sun and Stars" (Dulk 1985), and "High-Energy Neutral Radiations from the Sun" (Chupp 1984). Compared to these reviews, the present work necessarily requires a more narrow focus because of the greater bulk of the observational material. However, we attempt to put the high-energy particles in the context of the broader theoretical picture of the structure and dynamics of the solar atmosphere. Section 2 provides some background and describes the state of knowledge before about 1990. A brief summary of the observational tools, with mention of new data sources, is presented in Sections 3 and 4. Sections 5 and 6 comprise a topic-oriented discussion of new developments, and we conclude in Section 7 with comments about unsolved problems.

2. BACKGROUND

The subject of high-energy particles in solar flares presumably begins with the original observation of a flare by Carrington (1859), who noted the occurrence of a nearly simultaneous compass deflection at Kew Gardens. Prudently, he refrained from leaping to conclusions ("One swallow does not make a summer.") Had he done so, he might have inferred the existence of X radiation before Röntgen or the existence of the ionosphere before Heaviside! Instead astronomers heeded the advice of Lord Kelvin, who argued persuasively—on sound theoretical grounds—that any solar influence on a terrestrial compass needle was quite out of the question (Meadows 1970).

Matters have changed somewhat since the nineteenth century, and we have now a broader physical basis for understanding such phenomena. We can now

identify many populations of energetic particles created by solar flares. Here we use a broad definition of "flares" as both active-region flares and other forms of solar activity, such as coronal mass ejections (CMEs)[1] and various meter-wave radio bursts. These populations include the following:

- 10–100 keV electrons ("deka-keV" electrons),
- relativistic electrons ($E > 10$ MeV),
- 10–100 MeV ions,
- >100 MeV ions, and
- high-energy neutrons.

This review focuses primarily on particles in flares, citing the interplanetary observations only as necessary for understanding the physics. Energetic particles occupy a central position in solar flares and other forms of solar activity in the lower corona and below. In this region the particles accelerate to high energies, propagate, produce secondary effects, and then either thermalize or "escape." Because we wish to assess the present state of our knowledge of these particle populations, much of our discussion needs to be in terms of indirect remote-sensing observations (typical of astronomy) rather than direct in situ measurements (more typical of interplanetary physics and geophysics).

The core knowledge upon which the new developments in this field depend consists of the following elements. Solar flares (as broadly defined above) accelerate high-energy particles. The particles, both electrons and ions, can reach relativistic velocities relatively promptly (in a few seconds) and nearly simultaneously (Forrest & Chupp 1983). To a greater or lesser extent, particle acceleration is ubiquitous. It appears to occur in all flares, including relatively minor ones. In the 10–100 keV range, the electron component is significant in the overall energy budget, reaching 10% or more of the total (Lin & Hudson 1976). The most intense high-energy radiations (X rays and γ rays) come from closed magnetic structures in solar active regions[2] near sunspots, but these magnetic structures do not usually penetrate directly into the sunspot umbrae except for especially powerful flares. In gradual flares, with time scales exceeding an hour as observed in soft X rays or Hα, large systems of post-flare

[1]The association of coronal mass ejections with flares is presently a controversial subject. Gosling (1993) has suggested a "new paradigm" in which CMEs are actually the more fundamental part of the process and cause flares, via "post-CME" loops (Kahler 1992). The necessity for this point of view has been questioned by Hudson et al (1995), who point out that the physical processes involved in flares and CME-launching solar events (as seen in X rays and chromospheric effects) have long been known to have strong physical similarities (e.g. Harvey et al 1986).

[2]By "closed" we mean magnetic field lines that arise and loop back into the photosphere close to the point of origin, rather than extending out into the heliosphere as a part of the solar-wind flow.

loops form. Such flares are commonly associated with strong interplanetary phenomena such as shock-driven particle acceleration, CME launching, and major geomagnetic effects.

The time development of a solar flare is divided nominally into an impulsive phase and a gradual phase (Kane 1969); the former is characterized by intense deka-keV X-ray emission with a nonthermal spectrum, and the latter by soft X-ray emission with a thermal spectrum. Note that the terms "impulsive" and "gradual" may not be too relevant to the physics, because we know now that the nonthermal energy release in a gradual flare may itself be gradual (Hudson et al 1994a).

3. OBSERVATIONAL TOOLS

Because we cannot measure energetic particles in flares in situ, we rely on remote-sensing techniques. Fortunately, both electrons and protons have relatively direct radiative signatures, as discussed below. Besides the direct signatures, there are indirect signatures involving line profiles and polarization. We address these briefly after discussing the "mainstream" techniques of X-ray and γ-ray emissions. The indirect tools provide the only means for studying some parts of the particle spectrum, e.g. protons below about 10 MeV.

3.1 *Direct Signatures*

HARD X-RAY AND GAMMA-RAY CONTINUUM Hard X radiation ($h\nu > 10$ keV) from solar flares, first observed by Peterson & Winckler (1959), is the bremsstrahlung from nonthermal electrons. [Suggestions have also been made for "inverse bremsstrahlung," where energetic protons ($E_p \approx m_p/m_e \times E_e$, or a few MeV) produce hard X-ray photons by scattering ambient electrons (Boldt & Serlemitsos 1969, Heristchi 1986). However, this process conflicts with the measured γ-ray line fluxes (Emslie & Brown 1985, Hudson 1973). For a recent comprehensive discussion of proton and electron beams in solar flares, see Brown et al (1990).] The physics of the bremsstrahlung is relatively well understood (e.g. Koch & Motz 1959). The uncertainties in interpretation come mainly from the astrophysical environment. The electrons radiate either in the corona ("thin-target bremsstrahlung") or wherever they come to rest and thermalize ("thick-target bremsstrahlung") (Brown 1971, Hudson 1972). The same distinction applies to the ionic component. This distinction is useful in simplifying the theoretical treatment of radiation from particles trapped in loops, especially without spatially resolved observations. The observations show a continuum spectrum that may extend from the lower limit of detection (about 5 keV, limited by the bright background of the thermal soft X-ray sources) to tens of MeV (limited by sensitivity). This spectrum has a complex structure (sketched in Figure 1), indicating the presence of several acceleration processes or particle populations.

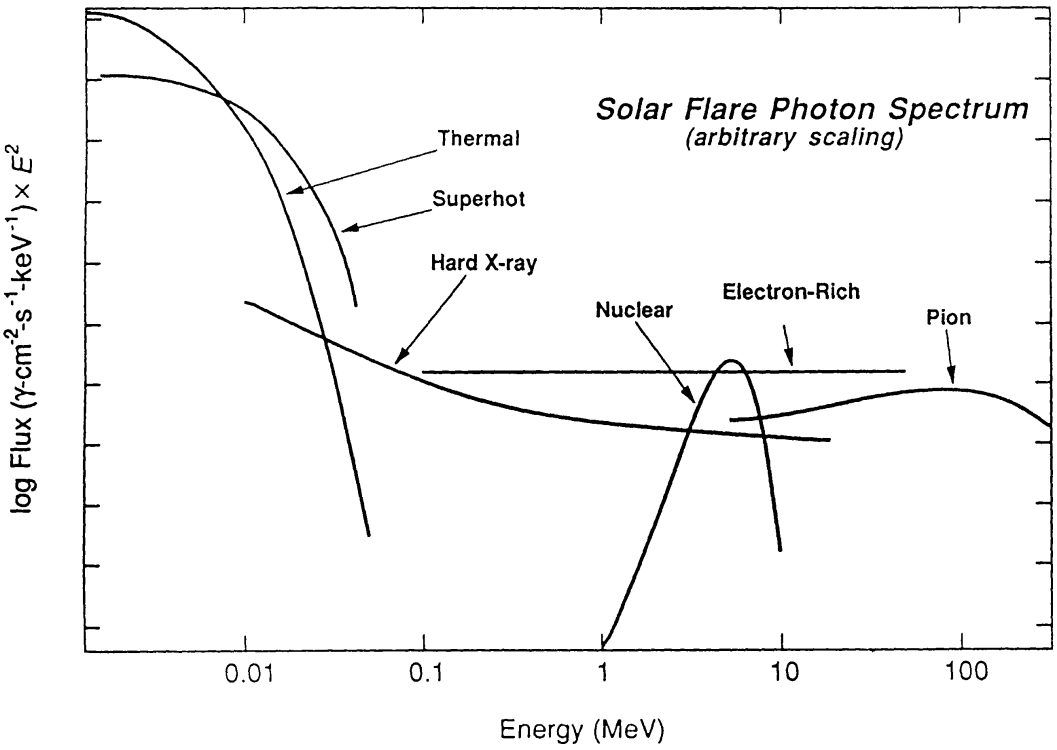

Figure 1 Sketch of the different components of the solar X-ray and γ-ray spectrum multiplied by E^2 to show power per energy decade: the spectrum of plasma radiation from typical loop sources in flares; similar spectrum of the "superhot" component; ordinary impulsive-phase broken power law; "electron-rich" or Rieger spectrum; γ-ray nuclear lines and continuum; and π^0 decay continuum. Note that these components are generally not simultaneous nor detectable in all events. For comparison, a similar figure in the Svestka monograph (1976) only showed three independent components.

Bremsstrahlung and atomic free-bound radiation represent the dominant emission mechanisms for this continuum from energies of tens of MeV down to the atomic bound-bound transitions, starting with the K transitions of Ni and Fe below 10 keV. At high energies there may be continuum from π^0 decay and secondary electrons from charged pion decay. Other continuum sources include positron-electron 3-photon annihilation, Compton backscatter, broadened nuclear lines, and detector effects. We mention the latter only to remind the reader that at high energies, the energy dispersion of the spectrometers is often quite broad. The polarization of bremsstrahlung radiation contains information about the beaming of the primary electrons (e.g. Bai & Ramaty 1978), but these polarization measurements are exceptionally difficult to make.

The hard X-ray emission of the impulsive phase appears to come mainly from the footpoints of closed magnetic field lines, in loops with rather small convergence (mirror ratio $B_{max}/B_{min}<5$) and relatively high magnetic field B (Petrosian 1994). The directivity of the bremsstrahlung would be a clue to

the anisotropy of any beaming that resulted from electron acceleration (Bai & Ramaty 1978), but no study has provided conclusive evidence for directivity (e.g. Li 1994, Vestrand et al 1987). We conclude that the electron transport may be more diffusive than beam-like (but see McTiernan et al 1994).

GAMMA-RAY LINES AND NEUTRONS Successful measurements of solar nuclear γ radiation, as evidenced by emission lines from deuterium formation (2.223 MeV), positron annihilation, and excited carbon, nitrogen, and heavier nuclei, began with the original detection by the *OSO-7* spacecraft (Chupp et al 1973), and blossomed with the measurements of the more capable Gamma Ray Spectrometer (GRS) (Forrest et al 1980) instrument on the *Solar Maximum Mission* (*SMM*). Recent instrumental improvements on *CGRO* are in the areas of spectroscopy, expanded energy range, and sensitivity, since imaging above 1 MeV (except indirectly by limb occultation, as described below) has not yet been achieved. Neutrons, first detected by the GRS, have been measured by *CGRO*, providing complementary information about the energetic proton spectrum at the Sun.

The types of γ radiation from solar flares are varied and the processes responsible for the emission can be complicated (Murphy et al 1987, Ramaty et al 1979). Protons (and heavier ions), once accelerated, scatter off ambient protons (and heavier ions). The velocity of the center of mass of the colliding particles determines how the γ-ray lines are Doppler shifted or Doppler broadened.

Many combinations of collisions among high-energy protons, alphas, and heavy nuclei (except proton-on-proton and heavy-on-heavy) yield nuclear lines, positrons (and subsequent 511 keV radiation), and/or neutrons (detected either as 2.223-MeV γ-ray photons, directly as free neutrons, or indirectly as neutron-decay protons in space). With all of these reaction channels and their associated emissions available, one would think that the spectrum and composition of the accelerated particles could be determined easily. This is not the case, however, largely because of the nature of the interaction cross sections. In practice one is restricted to determining only the general shape of the accelerated particle spectrum (Murphy & Ramaty 1984). The groups of reactions that commonly determine this general shape are those of collisionally excited nuclei and neutron spallation. The excited nuclei radiate in lines, mostly bunched in the region of 4–7 MeV. The excitation cross sections for these lines have thresholds typically in the 10–20 MeV range of primary energy per nucleon. The range of 4–7 MeV in γ rays is convenient because it has often only a small contribution from primary electron bremsstrahlung. The neutron production channel manifests itself in the narrow emission line at 2.223 MeV. Although the thresholds for producing free neutrons are also in the range of 10–20 MeV, the cross sections remain large even beyond 100 MeV, as opposed to nuclear γ-ray line cross sections that peak at energies not far above the threshold energy, i.e. 30–40 MeV. Thus, by comparing the fluence in the range of 4–7 MeV to that in the

2.223 MeV line one obtains a measure of the proton spectrum at widely different energies. Note that this comparison (and that for the delayed 511 keV line) requires fluences, not instantaneous fluxes, and this introduces considerable model-dependence in the theory.

For well-measured flares away from the limb the comparison of fluences of the 2.223 MeV and nuclear γ-ray lines allows only a surprisingly narrow range for the empirical proton-energy power-law spectral index $s = 3.9 \pm 0.4$ (Murphy & Ramaty 1984, Ramaty et al 1993).

PION-RELATED RADIATION If protons or heavier ions are accelerated to sufficiently high energies ($\gtrsim$300 MeV/nucleon), they are capable of producing both charged and neutral π mesons when scattering off ambient nuclei. The $\pi^+(\pi^-)$ meson decays successively into a $\mu^+(\mu^-)$ and then into an electron (positron) and neutrinos. The secondary electrons (positrons) in turn radiate by bremsstrahlung. Neutral pions, on the other hand, decay electromagnetically into two γ rays, each of energy 67 MeV (Doppler broadened). Other pion decay modes are rare ($<$1%).

The first unambiguous detection of solar radiation associated with pions was in the flare of 3 June 1982 (Figure 2) (Forrest et al 1985, 1986) and indicated that protons and/or ions were accelerated at least to energies approaching 1 GeV. High-energy neutrons ($\gtrsim$500 MeV) were also measured along with these γ rays in the GRS instrument (Chupp et al 1985, 1987) and indirectly in ground-level neutron monitors (Debrunner et al 1983, 1990). [Although high-energy neutrons were detected from the flare of 21 June 1980 (Chupp et al 1982) and one could infer the existence of free pions, the signal was much weaker than that of the 3 June 1982 flare.] Following the logic of the last section, the pion-related emission provides a large lever on the accelerated proton spectrum. A detection of pion-related emission by itself implies either a hard proton spectrum or the detection of an independent population of high-energy particles. Similarly, the ratio of the 4–7 MeV emission to the pion-produced component is sensitive to the shape of the spectrum at high energies.

Closely associated with pion-related γ-ray emission is the emission of high-energy neutrons detected at ground level with neutron monitors (Debrunner 1994). With an effective threshold of $\sim$200 MeV, neutron monitors sample the same (and higher) energies of the parent proton spectrum in a flare.

RADIO: MICROWAVES AND MILLIMETER WAVES There is a long and rich history of microwave observations of solar flares, extending back to the 1950s and earlier (Kundu 1965). Such observations show the presence of high-energy particles via synchrotron radiation in magnetic regions. Other emission mechanisms include free-free radiation (i.e. bremsstrahlung) thermal gyroresonance emission, and possibly transition radiation (Fleishman & Kahler 1992). The solar corona is generally optically thin to microwaves, except in strongly magnetized

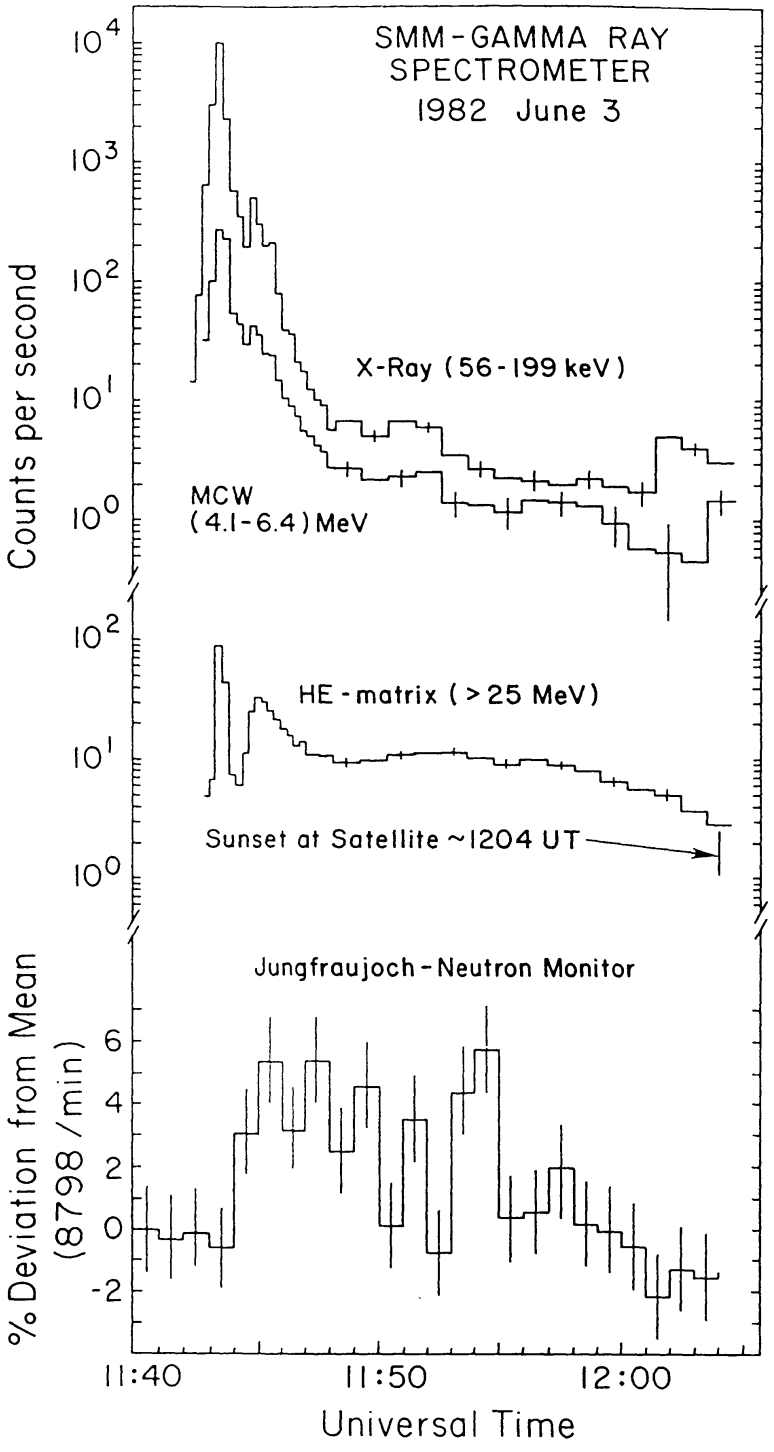

Figure 2 The flux-time profiles of the 3 June 1982 solar flare (Chupp et al 1987). The upper two curves are, respectively, the hard X-ray (50–200 keV) and nuclear γ-ray (4–6.4 MeV) count rate–time profiles. The middle curve is the count rate–time profile for events >25 MeV. This has contributions from both high-energy γ rays and neutrons. The peak at 1145 UT is due primarily to pion-related γ rays. The lower curve is the count rate–time profile of the Jungfraujoch neutron monitor (threshold of ~200 MeV).

or flaring regions. At millimeter wavelengths one can observe relativistic electrons through synchrotron emission, as well as thermal plasmas through free-free emission. The highest frequencies (>30 GHz) have not been well measured because 1. the background solar radiation creates a rapidly increasing background for low angular resolution observations and 2. there are few mm-wave telescopes capable of solar observation. New facilities (including the use of general instruments such as the Very Large Array or BIMA, and dedicated facilities such as Nobeyama or Owens Valley) have produced many important results that we cannot review in detail here. Because of the great sensitivity of the radio observations, many of these results do not yet have counterparts in the more difficult high-energy (hard X-ray and γ-ray) observations, even though they involve nonthermal particles of similar energies.

In the impulsive phase of a flare, we have an opportunity to make direct comparisons between radio and high-energy measurements. The particle energies and locations inferred from the microwaves agree largely with those inferred from the X-ray and γ-ray observations (Gary 1985). The comparison requires some knowledge of the flare geometry and the physics of electron transport: As long as the electrons are trapped, they can produce microwave emission, but if they radiate hard X rays they are lost from the system. The comparison favors the thick-target model (Lu & Petrosian 1989). A physical time scale arises from this comparison because of the trapping. Wang et al (1994) find, in one recently analyzed event, that the identification of the X-ray and microwave electrons as a single population requires a trapping time of a few seconds. This is roughly consistent with observations of impulsive bursts, which show delays of this magnitude (Cornell et al 1984).

RADIO: DECIMETER AND METER WAVES At lower frequencies ($\lambda > 10$ cm) the general comments made above also apply. The decreases in density and in the plasma-frequency cutoff restrict these observations to the high corona. In this domain one finds numerous dynamic effects (burst types I–V and others) attributable mainly to different types of nonthermal particles in different closed and open magnetic structures. Because of the low density of the corona, these phenomena can typically only be observed at radio wavelengths. The emission mechanisms become more complicated than at shorter wavelengths, with (for example) the possibility of radiation at the plasma frequency and its harmonic via coupling to electromagnetic radiation through Langmuir waves. Low-frequency radiation may be suppressed by synchrotron self-absorption, free-free or gyroresonance absorption from overlying cool material, plasma-frequency suppression, or the Razin-Tsytovich effect.

3.2 *Indirect Signatures*

WINGS OF LYMAN-α Low-energy protons and ions could be quite numerous and energetically important, but because they cannot excite γ-ray lines in nuclei

of carbon, nitrogen, etc, they are essentially invisible. Theorists over the years have noted various applications of such "sub-cosmic rays." Several researchers have pointed out that charge-exchange between low-energy protons and ambient neutral hydrogen could result in fast hydrogen atoms, which could produce detectable broad wings on, for example, Lyman-α (Brosius et al 1994, Canfield & Chang 1985, Orrall & Zirker 1976). In the solar case, our ability to image different parts of the flare at different times might make detection relatively straightforward. Solar searches for this effect (Canfield & Chang 1985, Canfield & Cook 1978) have been inconclusive, but there is an interesting UV observation of the flare star AU Mic interpreted in this manner (Woodgate et al 1992).

EMISSION LINE POLARIZATION Low-energy protons ($E < 10$ MeV) can also produce linear polarization in emission lines such as Lyman-α or Hα (Henoux et al 1990b) through impact. Such an effect would be expected in the presence of an intense beam of particles, as is needed to explain impulsive-phase energy release in a flare. Thus far, searches (Henoux et al 1990b, Metcalf et al 1994) have only begun to establish the existence of low-energy proton beams.

INTERPLANETARY OBSERVATIONS Observations of charged particles—indirectly at ground level initially and later in space directly—provided our first knowledge of solar high-energy astrophysics. This channel has been remarkably productive in providing information about solar processes, given the great uncertainties regarding particle transport from acceleration sites near the Sun. The interplanetary medium also puts its own imprint on the charged particle populations through shock acceleration and other effects.

Interplanetary particle events basically fall into two distinct categories: gradual and impulsive (Cane et al 1986, Kahler 1992, Reames 1992, Reames et al 1994). The former are characterized by their association with large and long-duration soft X-ray flares and coronal mass ejections; these have so-called normal (solar-wind-like) compositions. When measurable, the charge states of the ions reflect source temperatures on the order of $1–2 \times 10^6$ K. Impulsive events, on the other hand, are associated with small and short-duration flares (or with no detectable chromospheric flare) with elemental compositions rich in heavier elements, ^{3}He/^{4}He enhancements as large as 10^4, and high electron-to-proton ratios. Ion charge states in these events are representative of temperatures $>10^7$ K. The gradual event particles are ascribed to a coronal origin, as opposed to an origin within the flare environment. They are accelerated remotely by interplanetary shocks and have a seed population unaffected directly by the flare itself. Impulsive event particles are widely believed to originate from the flaring region of the corona. ("The flaring region" probably does not mean the actual loops that are bright in soft X rays in the sense that the particles actually escape from these loops. It appears more likely that the particles originate on open field lines near these loops. This point is somewhat controversial.) The

ionization temperatures in impulsive events are similar to the temperatures measured remotely with soft X-ray instruments, i.e. 10–30 $\times$ 10^6 K. There is also some evidence that the composition of these events is similar to that deduced from γ-ray measurements of flares (Ramaty et al 1993, Reames 1992).

ULTRAVIOLET-OPTICAL-INFRARED OBSERVATIONS (UVOIR) Many other ultraviolet, optical, and infrared radiations have direct associations with high-energy particles and thus provide clues to the properties of these particles. To make use of these observations in this sense, they must be interpreted in terms of a theory—usually a numerical model, because of the complexity of the structures and dynamics involved. Particle transport, radiative transfer, and magnetohydrodynamics are often studied independently in such numerical models, and it would be fair to say that we are quite far from having self-consistent theories including all of these (or other) elements.

The UVOIR observations of the lower atmosphere show its links to the corona, for example, in conduction-driven or particle-driven evaporation. There is considerable literature on observations relating the precipitation of deka-keV electrons to the evaporation of chromospheric material during the impulsive energy release: white-light continuum, UV flashes, and red-shifted Hα interpreted as momentum balancing for the evaporative flow (Acton et al 1982, Wülser et al 1994). Finally, there are strongly nonthermal phenomena thus far observed only in the UV, especially via high-resolution spectroscopy. These include jets and other explosive events (Brueckner & Bartoe 1983), which appear to involve physics distinct from that of flares and other larger-scale phenomena. Because of their scale, little is known about the behavior of high-energy particles in these environments.

4. NEW OBSERVATIONS

4.1 *Compton Gamma Ray Observatory*

The *Compton Gamma Ray Observatory* was launched in April 1991 (Gehrels et al 1993, 1994; Kniffen 1989a,b). The *Observatory* carries four instruments (Table 1) covering the energy range from 20 keV to 20 GeV. The instruments were designed to measure weak cosmic sources and are thus much more sensitive than either those on earlier spacecraft or on many balloon platforms. This also means that saturation effects may occur. A dedicated observation of the Sun allowed all the instruments on *CGRO* to record the remarkable flares of June 1991.

The BATSE (Burst and Transient Spectroscopy Experiment) instrument (Fishman et al 1989) is a spectrometer with large area and high time resolution. It measures hard X-ray and γ-ray transients over the full sky and thus serves as a monitor of solar hard X-ray emissions in addition to providing individual flare measurements. The OSSE (Oriented Scintillation Spectrometer

Table 1 Summary of *Compton Observatory* instrument properties

Instrument	Energy range	Time Resolution	Objectives
BATSE	20–300 keV	64 ms	full-sky transient detection
OSSE	0.05–10 MeV	2 s spectra; 16 ms (counter)	hard X rays and nuclear lines
COMPTEL	0.8–30 MeV[a] 0.6–10 MeV[b]	statistics limited[a] 12 s[b]	high S/N γ and neutron spectroscopy
EGRET	50–2000 MeV[a] 1–100 MeV[b]	statistics limited[a] 32 s[b]	high S/N γ and neutron spectroscopy

[a]telescope
[b]spectrometer

Experiment) instrument (Johnson et al 1993) is a spectrometer in the style of the γ-ray spectrometer on *SMM,* only with several times the sensitive area. With its large area it can monitor the behavior of γ-ray lines as a flare progresses.

The two other *CGRO* instruments, COMPTEL (Compton Telescope) (Schönfelder et al 1993) and EGRET (Energetic Gamma Ray Telescope Experiment) (Thompson et al 1993), are imagers operating in the range from 1 to 30 MeV and 50 to 2000 MeV, respectively. Besides performing spectroscopic measurements in these ranges, the imaging abilities of these instruments provide a high signal-to-noise ratio, thereby lowering the minimum detectable fluxes for neutrons, nuclear lines, and radiation associated with high-energy electron bremsstrahlung and pion decay. (Note, however, that the angular resolution of these telescopes is not good enough to resolve any individual features on the Sun.)

4.2 *Yohkoh*

The *Yohkoh* spacecraft was launched at the end of August 1991 (Ogawara et al 1991). It carries four instruments (summarized in Table 2) for high-energy observations and conducts simultaneous hard X-ray ($E > 13.9$ keV) and soft X-ray (1–2 keV) imaging at few-arcsec resolution. (For full descriptions of the instruments on board *Yohkoh*, see Vol. 135 of *Solar Physics.*) These imagers, plus spectroscopy experiments, make *Yohkoh* a powerful solar high-energy mission. Besides flares, *Yohkoh* (the soft X-ray telescope SXT in particular) also studies the structure and variability of the "quiescent" corona (e.g. Acton et al 1992a).

The *Yohkoh* flare observations are most relevant for this review. Following a trigger set by one of the instruments on board, typically a proportional counter responding to few-keV X radiation, a high-rate flare mode of operation delivers about 10 minutes of both high-time resolution and high-spatial resolution data. Between flares, most of the telemetry goes to full-Sun images from the soft

Table 2 Summary of *Yohkoh* instrumentation

Instrument	Energy range	Angular resolution	Objective
HXT	13.9–92.8 keV	~5 arc sec (synthesis)	hard X-ray imaging
SXT	1–3 keV	2.46 arc sec pixels	soft X-ray imaging
BCS	few keV		X-ray spectroscopy
WBS	X ray/γ ray		high-energy spectroscopy

X-ray telescope. The flare trigger threshold is typically at about the *GOES* C2 level ($\sim 2 \times 10^{-3}$ erg cm^{-2}s^{-1}), and less intense flares are recorded only in the normal SXT data stream plus the low-energy channel of the hard X-ray telescope HXT. In the first three years of operation more than a thousand flares were recorded.

5. NEW DEVELOPMENTS

5.1 *Long-Duration, High-Energy γ-Ray Flares*

One of the major discoveries of the *Compton Observatory* is a new class of flares with long-enduring, high-energy γ radiation. These are flares in which 50–100 MeV γ-ray emission, normally thought to be associated with π^0 decay, persists for periods of tens of minutes to hours. The same basic phenomenon was observed by the *Solar Maximum Mission* in the 3 June 1982 flare (Chupp et al 1987). During the 3 June 1982 flare, the γ-ray emission >25 MeV increased after the decline from the impulsive phase, while hard X-ray ($E < 100$ keV) and γ-ray fluxes (4–6 MeV) declined almost monotonically (Figure 2). These observations seem to require a distinct acceleration phase in addition to any impulsive phase acceleration (Forrest et al 1986). The acceleration in this late phase is quite efficient, accelerating protons to great energies without simultaneously accelerating deka-keV electrons and creating hot plasma as in the impulsive-phase acceleration.

In June 1991, active region NOAA #6659 transited the visible disk. Beginning with a major (X10) flare on 1 June while still behind the east limb (Barat et al 1994), this region produced five more flares at a level of X10 or greater on the NOAA soft X-ray classification scale (Ryan 1994). (An X10 flare causes an X-ray energy flux at the Earth of about 1 erg cm^{-2} s^{-1}, which is some 13 decades stronger than the fluxes from cosmic X-ray sources.) The most remarkable of these events occurred on 11 June 1991, when γ-ray emission

above 50 MeV persisted for at least 11 hours (Kanbach et al 1993), with the striking feature that most other flare emissions had ceased or subsided to undetectable levels long before this time (Figure 3). The detection of 2.223 MeV emission from deuterium formation also lasted more than 2 hours, establishing that the accelerated particles were indeed ions (Rank et al 1994, Ryan 1994) (Figure 4).

High-energy γ-ray and ground-level neutron emission was also detected for over one hour during the 4 June 1991 flare (Muraki et al 1992, 1994; Murphy et al 1994; Schneid et al 1994, Shibata 1994; Struminsky et al 1994a,b). The OSSE instrument on *CGRO* was able to monitor the dynamics of the γ-ray spectrum throughout the flare (Murphy et al 1993, 1994). One can see in Figure 5 that the high-energy particles were exciting carbon nuclei (4.43 MeV line) and producing neutrons (2.223 MeV line). Other occurrences of this include the 15 June 1991 flare in which γ-ray and neutron emission persisted for over one hour (Akimov et al 1991, Debrunner et al 1993b, McConnell 1994) and the 24 May 1990 flare, measured by the PHEBUS instrument on the *GRANAT* spacecraft (Terekhov et al 1993, Vilmer 1994). Ground-level neutron monitors measured neutrons from this flare (Debrunner et al 1993a, Kocharov et al 1994, Shea & Smart 1991, Vilmer 1994). Figure 6 shows the count rate from the Climax neutron monitor; the first increase is attributed to solar neutrons, while protons

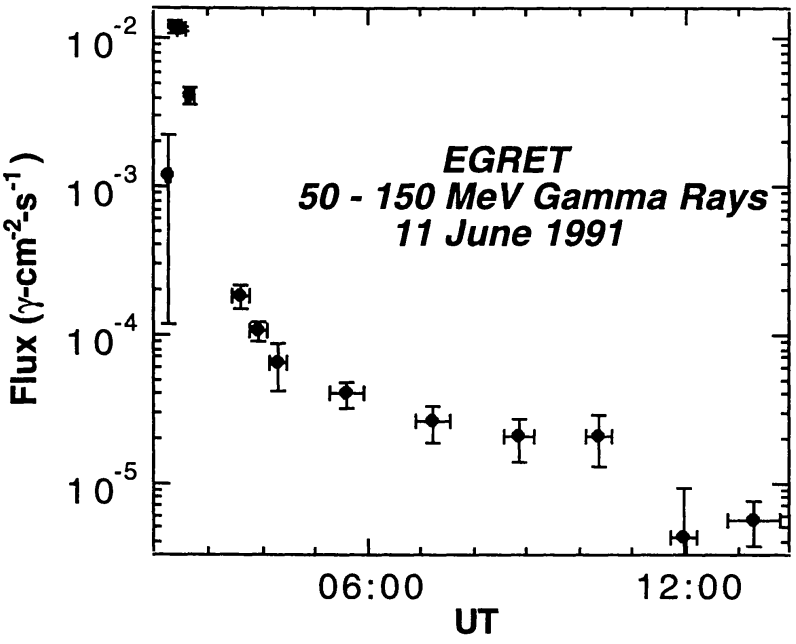

Figure 3 Time variation of 50–150 MeV γ rays during the 11 June 1991 flare (Kanbach et al 1993, Schneid et al 1994), as observed by the EGRET instrument on board the *Compton Gamma Ray Observatory*. The unprecedented duration of this radiation implies either long-duration particle storage in the solar corona, analogous to the Van Allen radiation belts of Earth, or else high-energy particle acceleration continuing well after the flare impulsive phase.

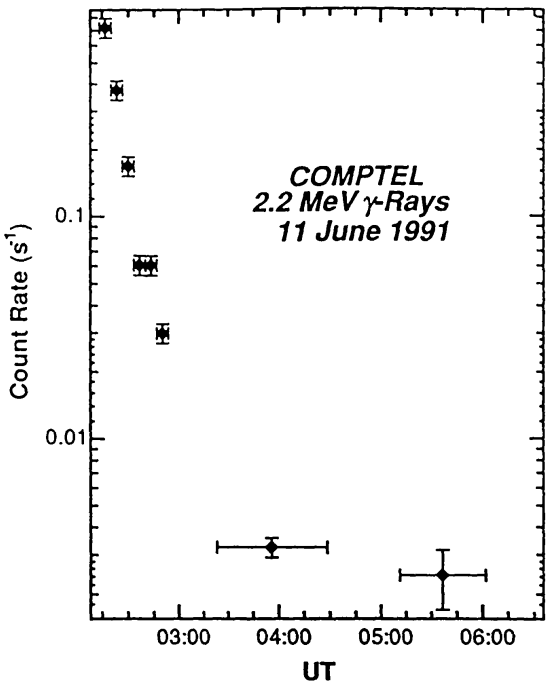

Figure 4 Time variation of 2.223 MeV γ rays during the 11 June 1991 flare (Ryan et al 1993). The presence of this line (with a decay constant similar to that in Figure 3) establishes that the high-energy protons responsible for the neutron secondary radiation persist long after the impulsive phase of this flare.

are responsible for the second increase (Debrunner et al 1993a, Shea & Smart 1991). Careful analysis of *SMM* high-energy γ-ray data indicates that there have been other occurrences of this phenomenon during the most recent solar maximum (Dunphy & Chupp 1994).

5.2 *"Electron-Rich" Flares*

Solar flares or individual bursts within solar flares sometimes can have an unusually intense bremsstrahlung spectrum, enough to obscure the γ-ray emission lines. The term "electron-rich γ-ray flares" describes this phenomenon, which was discovered with *SMM* (Rieger & Marschhäuser 1990). The main characteristic of these events is a γ-ray continuum spectrum largely deficient in nuclear lines, presumably bremsstrahlung from primary energetic electrons, extending up to a few tens of MeV. These events have short durations (a few to a few tens of seconds) (Pelaez et al 1992, Yoshimori et al 1992, Marschhäuser et al 1994, Rieger 1994). Two such impulsive events were well measured by *CGRO*: 30 June 1991 and 2 July 1991 (Dingus et al 1994, Ryan 1994). Neither flare was exceptionally large on the thermal X-ray flux scale (M class), but both exhibited intense continuum γ-ray emission. The spectra of both these flares were well fit by power laws in energy, $(h\nu)^{-2}$, with small contributions of nuclear lines at the usual energies (Figure 7). Few attempts have been made to address the

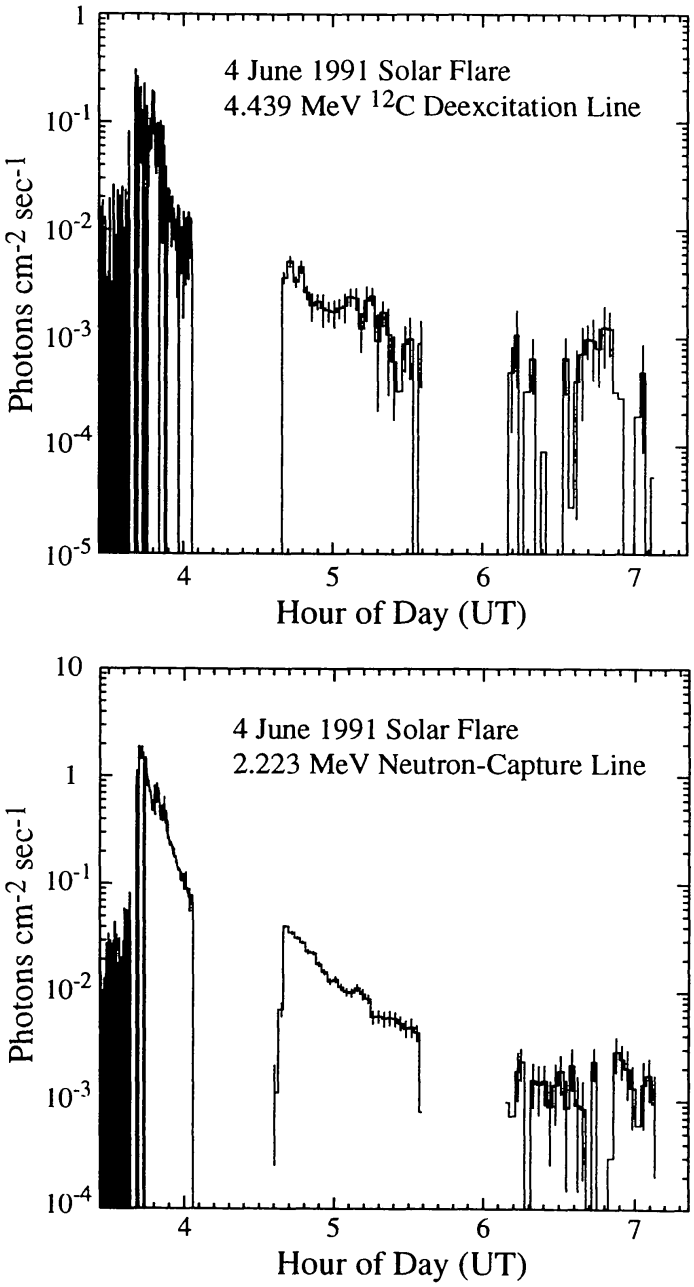

Figure 5 Time variations of 2.223 MeV (neutron capture; *top panel*) and 4.44 MeV (^{12}C deexcitation; *bottom panel*) following the 4 June 1991 event, again illustrating the extraordinary duration of the high-energy processes (Murphy et al 1994). These line measurements were accompanied by a time-extended detection of solar neutrons at ground level (Struminsky et al 1994a).

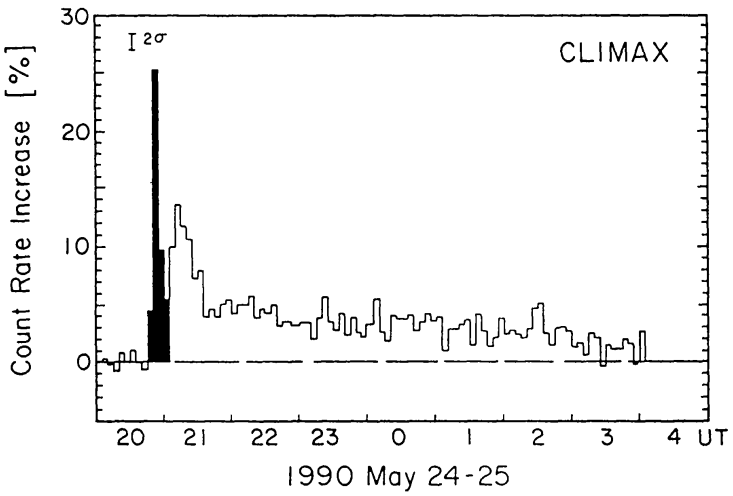

Figure 6 Neutron-monitor measurements of the 24 May 1990 flare showing evidence of high-energy (>200 MeV) neutrons striking the top of the atmosphere (Debrunner et al 1993a, Shea & Smart 1991). The first spike is due to solar neutrons; the later enhancement is due to solar protons (traveling a longer distance along the interplanetary magnetic field lines).

nature of these events, i.e. the variability of the electron/proton (ion) ratio in accelerated particles (see Section 6.2).

5.3 *Spectroscopy of Solar Neutrons*

Solar neutrons were detected by the GRS (Chupp 1990, Chupp et al 1987) and the Jungfraujoch neutron monitor (Debrunner et al 1990) during the flare of 3 June 1982 (Figure 8). The count rate of gamma rays with $E > 25$ MeV has been deconvolved into an impulsive burst of γ rays, a real delay, then a burst of γ rays of pion origin. The detection of neutrons with energies >50 MeV followed (Chupp et al 1987, Forrest et al 1986). A comparison of the neutron flux level measured in space with that measured on the ground essentially defines the overall spectral shape with two broadband points. From these data one can conclude that the accelerated proton spectrum extended beyond 1 GeV and was produced over a period of time well after the impulsive phase. These pioneering analyses arose from the synthesis of all the data, i.e. the nuclear lines from heavy nuclei, the 2.223 MeV line, and neutrons detected by spacecraft—both directly and via neutron-decay protons created on field lines well connected to an interplanetary spacecraft (Evenson et al 1983, 1990)—and at ground level (Debrunner et al 1983, 1990). The timing of these radiations and their existence established that the 3 June 1982 flare consisted of an intense and high-energy impulsive phase followed by a distinct and even higher energy delayed phase.

Most conveniently, solar neutrons fill in gaps in the unknown proton spectrum. As discussed above, nuclear γ-ray lines most strongly represent the few tens of MeV proton energy range, while the pion-related radiation represents

the number of protons (or ions) in the range of a few hundred MeV (Murphy et al 1987). Neutrons detected by space instruments, e.g. 20–100 MeV with COMPTEL (Ryan et al 1992), come from a region of the proton spectrum that lies somewhat higher than the nuclear lines and below that of the pion-related emission. Neutrons detected at ground level can reflect the proton population well above 500 MeV (Debrunner 1994). The ability to deduce the proton spectrum above ~20 MeV is limited when based solely on the γ radiation. One can use the details (i.e. the width) of the 70 MeV line emission as an indicator of the spectrum (Alexander et al 1994), but this is not as conclusive as directly measuring neutrons at these energies.

The COMPTEL instrument with its ability to measure the energy of individual neutrons has contributed to the understanding of two recent flares. The impulsive flare of 9 June 1991 emitted solar neutrons that were measured by COMPTEL (Ryan et al 1994a). The total neutron signal was small compared to that of the 3 June 1982 flare, but had the similarity that the bulk of the neutron emission occurred after the impulsive phase. The EGRET instrument detected γ-ray emission >20 MeV after the impulsive phase as well (Schneid et al 1994), at a time somewhat later than the neutrons detected with COMPTEL. These two observations lead one to conclude that high-energy proton acceleration often occurs in a separate and delayed phase of the flare.

The 15 June 1991 solar flare occurred in the same active region as that of 9 June 1991, but after the region had rotated from near the central meridian to the west limb. High-energy γ-ray emission approaching 1 GeV was detected starting ~17 minutes after the impulsive phase by the *GAMMA-1*

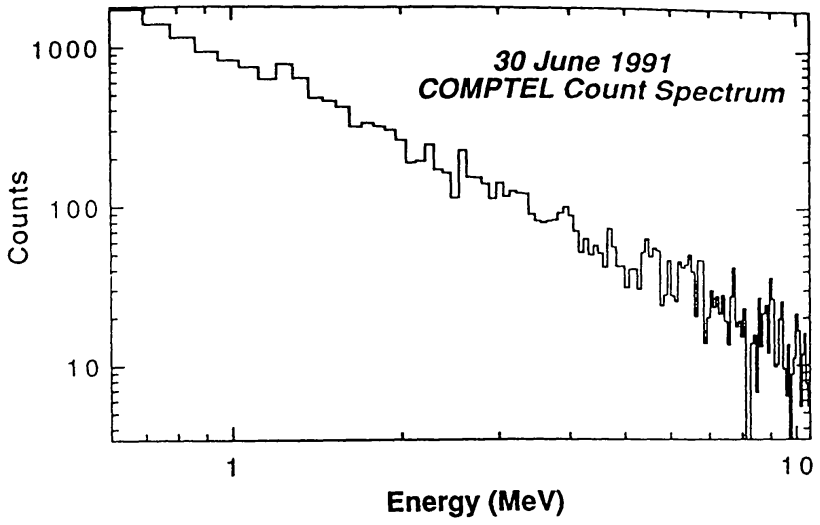

Figure 7 Spectrum of the 30 June 1991 flare in the γ-ray line region (Ryan et al 1993), showing how the bremsstrahlung continuum dominates in an "electron rich" event. Note the absence of a drop at about 7 MeV, where the strong γ-ray lines normally disappear.

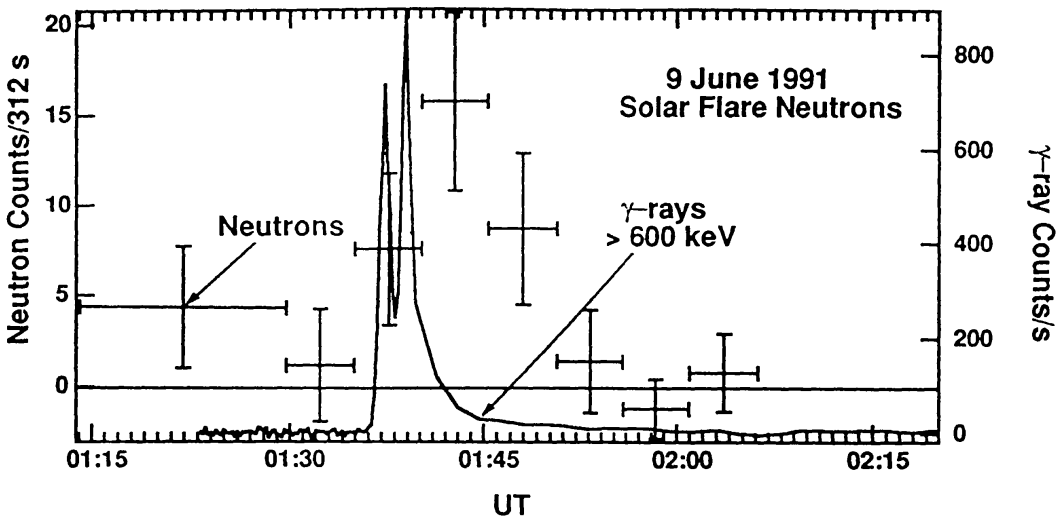

Figure 8 Neutron and γ-ray emission time profiles for the 9 June 1991 event observed by *CGRO*/COMPTEL, plotted at the time corresponding to a photon arrival time (Ryan et al 1994a). Errors from time-of-flight are about 1–3 minutes, so that these data confirm that the release of high-energy neutrons from the Sun followed the impulsive phase.

spacecraft over two 90-minute orbits (Akimov et al 1991, 1994). Similarly, the COMPTEL instrument, which started the observation ~40 minutes after the impulsive phase began, measured nuclear line emission for more than 50 minutes (McConnell et al 1993). Neutrons were also measured with the COMPTEL instrument. This instrument can independently measure neutron energies via time-of-flight and, given the subluminal speeds of these particles, they can be mapped back almost to the impulsive phase epoch. Such neutrons provide the only high-energy data from those epochs (Debrunner et al 1993b). For the 15 June flare the neutron spectral shape and its magnitude were found to be consistent with the nuclear-line and high-energy γ-ray data over the period of extended emission.

5.4 *Large Area γ-Ray Flares*

The solar flare of 29 September 1989 is important primarily because of its location on the Sun—it was approximately 10° behind the west limb. However, the γ-ray spectrum shows a distinct emission line at 2.223 MeV that is characteristic of a flare with a heliocentric longitude less than 70°. This is anomalous in that the deuterium line is heavily limb-darkened (Hua & Lingenfelter 1987). The simplest interpretation requires a spatially extended precipitation of flare-accelerated protons giving rise to γ-ray emission over a wide region of the Sun (Vestrand & Forrest 1993). Interestingly, not every large flare exhibits this property. Other limb events such as that on 27 April 1981 show no significant line from deuterium formation (Murphy et al 1990), indicating that the proton precipitation is largely restricted to the limb region. Likewise, even the large

flare of 1 June 1991 measured by the PHEBUS instrument (Barat et al 1994) does not show any evidence for such a large spatial extent. However, the single unambiguous occurrence of this phenomenon indicates that large parts of the solar corona are involved in the transport and perhaps the acceleration of protons in flares. Recently analyzed radio data indicate that multiple magnetic structures were also involved in the long-duration 3 June 1982 flare (Trottet et al 1994). This topic arises again later in this review.

A special class of gradual hard X-ray events (Hudson 1978) can also be interpreted in terms of large-scale trapping structures. These events are distinguished by flat hard X-ray spectra that harden with time, low microwave peak frequencies, and association with interplanetary particle events and metric type IV or continuum emission (Cliver et al 1986). The use of the solar limb as an occulter reveals, in extreme cases, that the source heights may exceed 10^5 km above the photosphere (Kane et al 1992) (Figure 9). There seems little doubt that these sources represent extremely large-scale magnetic loops capable of trapping electrons and protons for extended periods of time, presumably limited by processes similar to those in the magnetosphere, i.e. particle drift and scattering into the loss cone.

5.5 *The Neupert Effect*

The term "Neupert effect" describes the approximate match in time between the time integral of the microwave impulsive burst and the soft X-ray light curve of a flare (Neupert 1968). Generalized slightly, it describes the usual temporal relationship between the impulsive and gradual phases of a flare (Dennis & Zarro 1993). The easiest interpretation is simply that the impulsive-phase emissions, such as hard X rays, are closely associated with the energy release in a flare. Moreover, it implies that much of the thermal phase of the flare is an atmospheric response to energetic particles or to the process that accelerates the particles. The community is divided on this interpretation, even though the relationship identified originally by Neupert certainly prevails in most flares. The following comments describe related phenomena.

Previous observations had established the close association of flares with closed magnetic flux tubes to "footpoints" in the chromosphere. The acceleration of 10–100 keV electrons in these magnetic structures during the impulsive phase of a solar flare is a well-known result (Hoyng et al 1981). The HXT instrument on *Yohkoh* observes this population well, with imaging in four energy channels as described above. *Yohkoh* observations have completely confirmed the "impulsive footpoint" result of *SMM* (Duijveman et al 1982, Hoyng et al 1981) that the impulsive-phase hard X rays come largely from the footpoints of coronal magnetic loops. The footpoints may have comparable brightnesses. However, in cases where the two footpoints of the flaring loop can be identified with magnetographic observations of **B**, there tends to be a brightness asymmetry (Sakao 1994): The weaker field has the brighter hard X-ray emission, as one

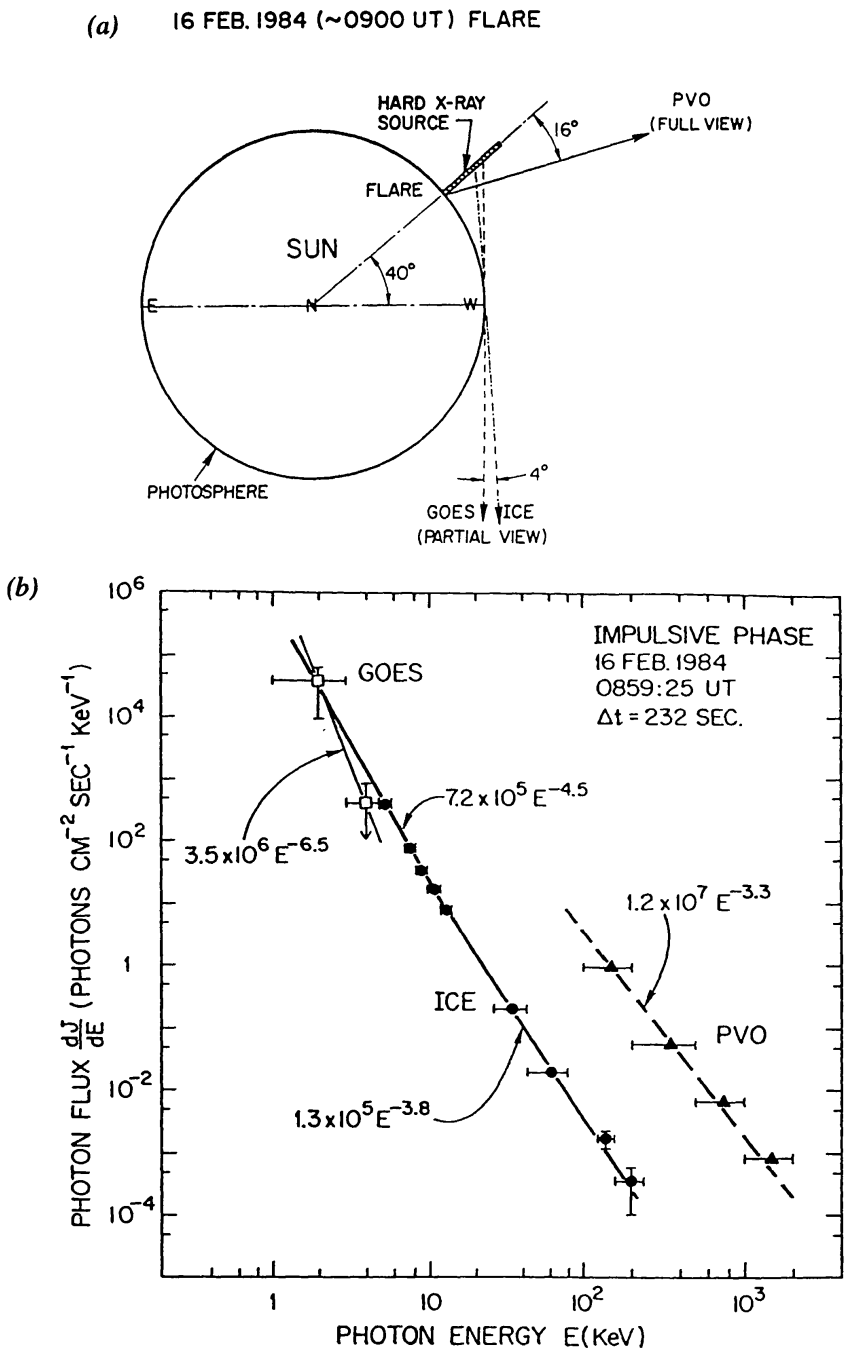

Figure 9 *(a)* Sketch illustrating the technique of limb occultation to separate the coronal emission from the brighter sources at lower altitudes (Kane et al 1992). In this case, the coronal sources (observed by spacecraft near the Earth) could be distinguished from the main radiation sources (observed by the *Pioneer Venus Orbiter*) for a flare some 40° behind the limb, corresponding to an occultation height on the order of 10^5 km. *(b)* Hard X-ray spectra observed at the two locations.

would expect from the mirror geometry of electrons bouncing adiabatically in a coronal flux tube (Nitta et al 1989). Moreover, Sakao (1994) finds that the footpoint sources are nearly simultaneous in time (with time differences typically on the order of 0.2 sec, implying exciter speeds greater than 5×10^4 km s^{-1} for loop dimensions of 10 Mm), a result that excludes transport mechanisms other than energetic electrons in coronal loops. Figure 10 illustrates this simultaneity. Thus, the *Yohkoh* results confirm, rather unambiguously, the existence of a powerful electron acceleration on closed field lines. The simultaneity of the footpoint brightenings is not yet known precisely enough to localize the actual point of acceleration along the loop.

In soft X rays, the *Yohkoh*/SXT images allow us to resolve the Neupert effect variations spatially. Generally, the tops of the loops have gradual variations and the footpoints have impulsive variations that closely follow the hard X-ray footpoint brightenings (Hudson et al 1994c, McTiernan et al 1993). Figure 11 illustrates how footpoint brightenings in a complicated multiple-loop flare appear in hard and soft X rays.

Yohkoh/SXT has also given us a more systematic look at white-light flaring, and this also supports the overall Neupert effect/evaporation scenario. *Yohkoh* typically returns five or six white-light images per minute during flare mode, centered on the brightest X-ray point. Many white-light flares have been detected (Hudson et al 1992, 1994b) and essentially all the major flares show visible continuum emission. These data confirm ground-based results (e.g. Neidig & Kane 1993) and clearly establish the simultaneity of one component of the white-light emission with the hard X rays that mark the precipitation of 10–100 keV electrons accelerated in the impulsive phase (Hudson 1972). Figure 12 shows the match between hard X-ray footpoint sources and white-light emission patches for a flare of 15 November 1991. However, not all components of white-light emission are associated with energetic particles (Ryan et al 1983). This process also suggests the occurrence of "black light flares" (Henoux et al 1990a), by a mechanism involving opacity variation driven by the electrons before they can cause appreciable heating. The SXT white-light observations have not yet succeeded in detecting this, presumably because of inadequate time resolution (Van Driel-Gesztelyi et al 1994).

Finally, the presence of the evaporative flow produces blueshifts in soft X-ray emission lines. The *Yohkoh* data generally confirm the close association of blueshifts with hard X rays, consistent with the scenario of the Neupert effect (Bentley et al 1994), although blueshifts outside the impulsive phase might be expected and may have been detected (Cheng et al 1994). It also appears that detailed numerical modeling of impulsive-phase evaporation has not caught up with the observations, because the models (Antonucci et al 1993) imply nonthermal electron spectra that are significantly softer than those observed.

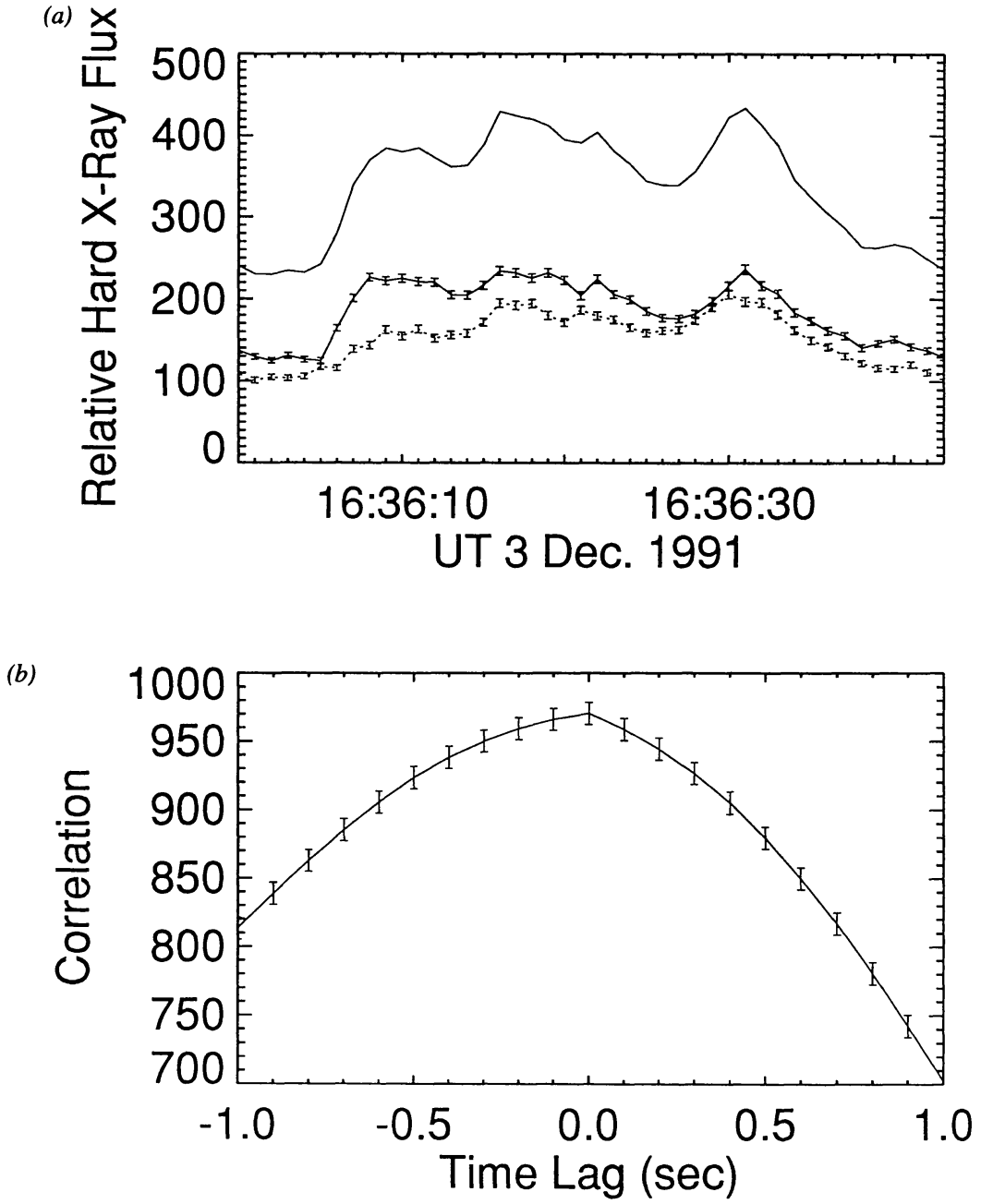

Figure 10 Illustration of the simultaneity of footpoint brightening in one of the flares observed by the hard X-ray imager on *Yohkoh* (Sakao et al 1994). *(a)* Individual brightness of the two footpoint sources derived from fitting Gaussian source models and their sum. *(b)* The cross-correlation between the two footpoint sources. The estimated delay between the two sources is <0.2 sec.

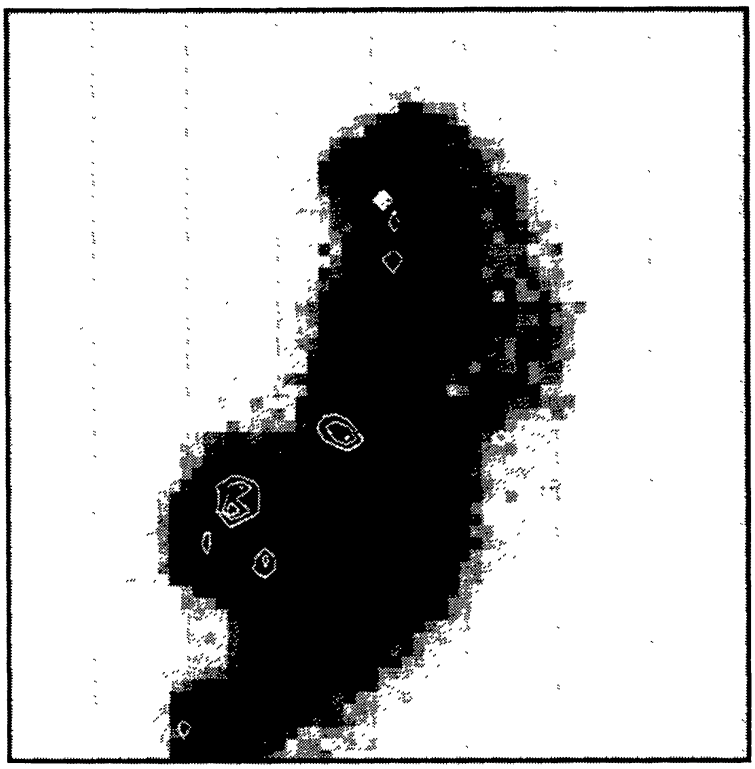

Figure 11 Footpoint brightening seen in soft X rays by the *Yohkoh*/SXT in a flare of 26 January 1992 (Hudson et al 1994c). The continuous tones represent soft (~1 keV) X-ray brightness, and the contours represent hard (33–53 keV) X-ray brightness. They both show a patchy character with some common features. This pattern is typical of most flares during the impulsive phase and tends to confirm the occurrence of particle-driven evaporation during the impulsive phase of the flare. The pixel size is 2.46″. N is up and E is to the left. The flare occurred near the SW limb in a region almost totally devoid of sunspots.

We should point out that counterexamples of the Neupert effect certainly occur, and these are of great intrinsic interest because the physics presumably differs in these cases. We are unaware of any published literature on these exceptions as such (but see Feldman et al 1994), but they probably include the "superhot" events described below and the extended high-energy events (e.g. Cliver et al 1986). However, because so many flares obey this simple sequencing of the impulsive phase riding on the leading edge of the soft X rays, the Neupert effect undoubtedly has a root physical cause that must closely resemble in effect the scenario offered above.

5.6 *Coronal Impulsive Hard X-Ray Sources*

In one of the most striking observations from *Yohkoh*, the HXT has detected remarkably bright hard X-ray sources in the corona above solar flares, with time variations that match those of the impulsive footpoint sources (Masuda et al 1994; see also Takakura et al 1993). Figure 13 shows the best example: a limb flare of 13 January 1992 (see also Hudson 1994). The location of this

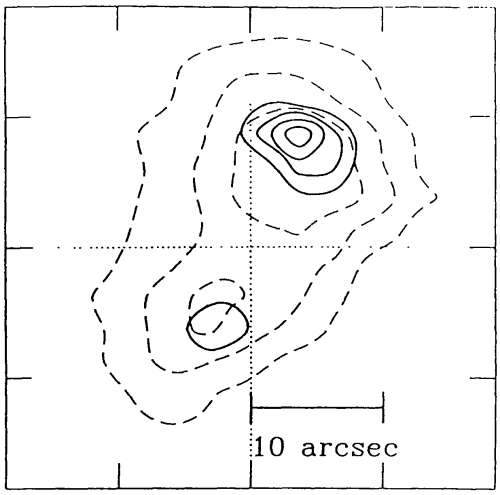

Figure 12 White-light emission patches (*dashed contours*) at the footpoints of the loop structure of the 15 November 1991 flare, as observed at 4308 Å with the *Yohkoh*/SXT instrument. The overlay shows the position coincidence with the hard X-ray sources (*solid contours*) detected by *Yohkoh*/HXT (Sakao et al 1992), establishing the penetration of nonthermal electrons deep into the chromosphere.

source strongly reminds one of the cusp geometries seen in many gradual soft X-ray flares and nonflare sources and provides almost unmistakable geometrical evidence that a neutral-sheet "helmet streamer" configuration plays a role in impulsive-phase particle acceleration (see below).

The noteworthy feature of these "loop top" impulsive hard X-ray sources is their very existence. They are surprisingly bright, considering the low density of the corona, and they are remarkably short-lived—a property normally associated with thick-target processes (Brown 1971, Hudson 1972). As of the literature cutoff date of this review, little serious theoretical work has appeared. To produce high luminosity in a medium with low density requires trapping (in order to approach the limit of a thick target), but the particles cannot be allowed to remain trapped long enough to cause emission delayed with respect to that of the impulsive footpoint sources. Alternatively, the density may be high enough to produce sufficient luminosity ($\sim 10^{12}$ cm^{-3}), but there is no evidence for high densities at the site of the impulsive hard X-ray source. For the loop-top source of the 13 January event, Masuda (1994) estimates a density of 3×10^8 cm^{-3} at a temperature of 2×10^8 K, which corresponds to a gas pressure of some 20 dyne cm^{-2}. This pressure does not seem dynamically unreasonable for the source altitude of some 2×10^4 km above the photosphere. The radiating plasma could conceivably be trapped in the low-pressure zone of the actual reconnection. In interpreting the impulsive loop-top hard X-ray source as thermal, however, there is a serious problem with the time scale: The electron thermalization time for Coulomb collisions can be estimated as $\tau_{ee} = (6 \times 10^6) T_6^{1.5} n_e^{-1}$, where T_6 is the coronal temperature in units of 10^6 K and n_e is the electron number density (cm^{-3}). For the parameters Masuda estimates, this time (about 60 s) significantly exceeds the variability time scale observed. The radiative time scale for an isothermal plasma presents a similar problem. Thus, at the time of this writing, the theoretical interpretation of the *Yohkoh* coronal impulsive hard X-ray sources remains poorly understood.

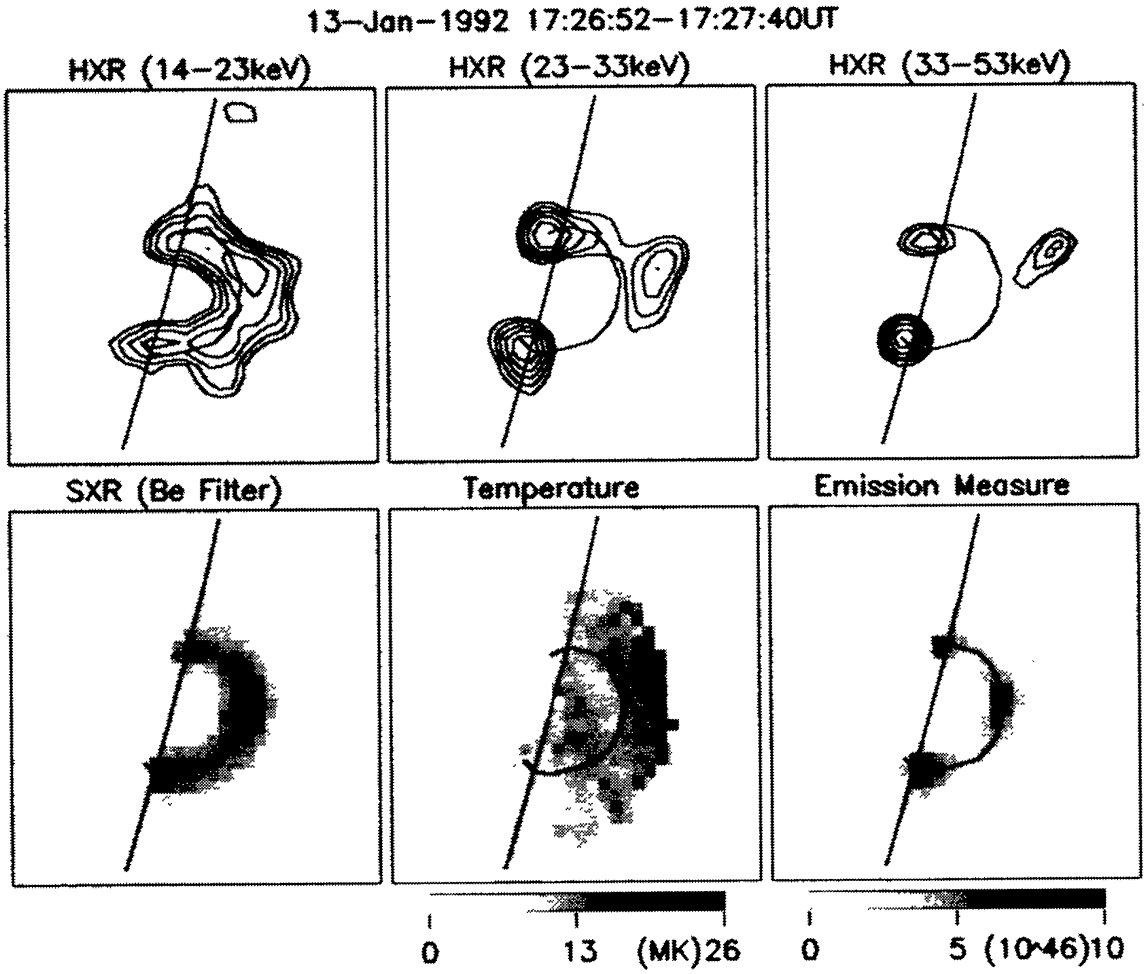

Figure 13 Discovery of a remarkable class of impulsive hard X-ray sources in the corona above the flaring loops for a flare of 13 January 1992 (Masuda et al 1994). The upper panels show contours of hard X-ray emission in the three lower-energy bands of the *Yohkoh* hard X-ray telescope. Note the coronal source above the loop, as traced by the solid line, in the upper right panel. The lower panels show the soft X-ray brightness, temperature, and emission measure distributions. The highest temperature appears at a point near the coronal hard X-ray source. Both hard X rays and soft X rays show the normal footpoint impulsive-phase sources. The pixel size is 2.46″.

5.7 *"Impulse Response" Flares*

The advent of mm-wave interferometric telescopes has produced some remarkable discoveries. Figure 14 illustrates two of them: the unprecedented flatness of the spectrum, which is almost constant in flux density (cf White et al 1992, Hachenberg & Wallis 1961) out to 86 GHz, and the characteristic fast rise–slow decay variation, with an exponential decay time constant of 20–30 s. We know of no viable theory yet for these events (White et al 1992). If (as one normally assumes) the mm-wave flux comes from gyrosynchrotron radiation, it implies MeV-range electrons with an extremely flat spectrum, $\delta \propto 1.4$, for $N(E) \propto E^{-\delta}$. Furthermore, this electron spectrum implies a photon spectral index $\gamma = 0.4$ in a thick target (e.g. Hudson et al 1978). The hardest solar hard

X-ray bremsstrahlung spectra are on the order of $\gamma = 2$, as in the electron-rich events (Rieger & Marschhäuser 1990). Nevertheless, a nonthermal explanation seems more likely because the thermal alternative (free-free emission) makes a clear prediction for a burst of soft X-ray emission that is not observed in these cases. We speculate on the basis of these data that they may show a wholly new population of accelerated electrons that arises in compact loop structures, near the level of the photosphere or imbedded in it. We also speculate that these brief events have a relationship with the electron-rich continuum events (see above).

5.8 *The "Superhot" Component*

The "superhot" component of hard X-ray emission comes from a hotward extension of the differential emission measure distribution of the normal soft X-ray sources, as observed with whole-Sun detectors, and is produced by low-energy (tens of keV) electrons. The original discovery used high-resolution Ge hard X-ray detectors (Lin et al 1981), which clearly established the exponential continuum spectrum characteristic of a thermal plasma. The *Yohkoh* imaging capability has now been used to show that the morphology of this kind of source

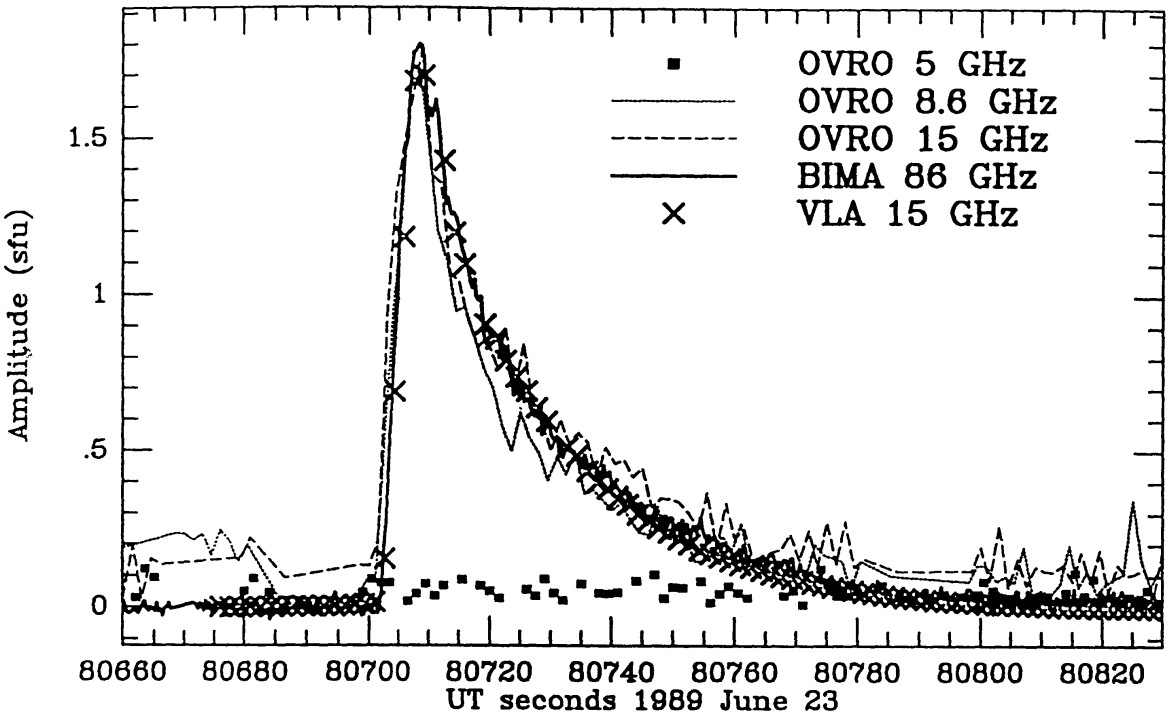

Figure 14 "Impulse response" flare observed at cm-mm wavelengths (White et al 1992). The two remarkable characteristics of this burst are its remarkably flat spectrum, with an abrupt low-frequency cutoff; and its time profile, repeated almost exactly in an entire class of events (White 1994). In this plot the different wavelengths (from three different radio observatories) have been normalized to one another, but the total variation of flux density across the entire range was within a factor of two.

differs strikingly from that of ordinary flare loops. In the "superhot" sources, the soft X-ray evolution gives the appearance of a slow filling of a magnetic loop by a cloud of hot plasma (Culhane et al 1994, Kosugi 1994, Sterling 1994), rather than the early footpoint/late loop-top pattern of ordinary flare loops that follow the Neupert effect.

The behavior of the superhot sources in these cases focuses attention on the basic question of the particle distribution functions. The energy input in these cases may be a simple form of heating, rather than the usual situation in which particle acceleration mediates the heating and results in power-law bremsstrahlung spectra. This distinction between heating and acceleration follows naturally in theories involving dc electric fields (Benka & Holman 1992, Holman 1985, Tsuneta 1985).

5.9 *Cusp Geometries*

The SXT images often show the presence of cusped "helmet streamer" configurations of the soft X-ray sources. While not associated directly with high-energy particles except for the evidence presented in Section 5.6, this geometry may be fundamental to flare physics. The existence of a cusp geometry is direct evidence for neutral-sheet formation in the corona with oppositely directed field lines extending approximately parallel to one another. These field lines may connect back to the photosphere, rather than open into the interplanetary medium (Tsuneta et al 1992). Note, however, that the resolvable spatial scales greatly exceed the theoretical thicknesses expected for coronal neutral sheets. SXT sees this structure clearly in many LDE (long-decay event) situations (Tsuneta et al 1992) (Figure 15). Earlier *Skylab* observations (e.g. Sturrock 1980) and even ground-based observations (e.g. Hanaoka et al 1986) had suggested the existence of this geometry, but the SXT data make it quite obvious. The cusp itself is not always present in the flare images, but there is also a clear tendency for overly bright structures near the tops of loops or arcades of loops to form (Acton et al 1992b, Feldman et al 1994). Here "overly bright" means in excess of the loop-top brightening that one would expect from ordinary conductive/radiative equilibrium (e.g. Rosner et al 1978) or from line-of-sight effects in the optically thin soft X-ray sources. In many cases, these cusped sources are passive and often exist outside flare situations. Accordingly, the SXT data by themselves leave open the question about the dynamics of the reconnection in the neutral-sheet geometry as an explanation for solar flares. Uchida et al (1994) offer an alternative reconnection scenario.

The HXT loop-top impulsive sources mentioned above (Masuda 1994) may provide the missing link that connects the physics of the gradual and impulsive flares. Although the hard X-ray images do not actually show a cusp configuration, they do show the existence of impulsive sources above the soft X-ray loop tops at about the location expected for a cusp. The time variations of these sources match those of the footpoint sources and therefore reflect the energy

Figure 15 *Yohkoh*/SXT image of a long-duration flare of 21 February 1992, showing clearly the helmet-streamer configuration only hinted at by the hard X rays for the impulsive flare shown in Figure 14 (Tsuneta et al 1992). With this cusp geometry there is no question about the validity of the helmet-streamer reconnection scenario. The pixel size is 2.46″.

release mechanism. This suggests strongly that the energy release is taking place in the neutral-sheet structure of the cusp or in close relationship to it. Accordingly, this result opens up the strong possibility that such a reconnection scenario, envisioned by many authors (Carmichael 1964, Hirayama 1974, Kopp & Pneuman 1976, Sturrock 1966), may apply not only to LDE events but also to compact flares as well.

5.10 *γ-Ray Line Spectroscopy*

As mentioned earlier, most nuclear deexcitation lines derive from a limited part of the accelerated proton spectrum (20–50 MeV). An analysis of the many line intensities from a solar flare is thus more sensitive to the compositions of the solar atmosphere and the accelerated ions than to the shape of the accelerated ion spectrum. With the daunting number of potential lines, both narrow and Doppler-broadened, and the underlying electron bremsstrahlung continuum, the analysis of even a well-observed flare is challenging (Murphy et al 1990). However, the analysis of the 27 April 1981 flare yielded some interesting conclusions (Murphy et al 1991). The composition of the accelerated ions (producing the Doppler-broadened lines) resembles more closely the composition of impulsive interplanetary particle events with large ^{3}He abundances than that of long-duration particle events. Murphy et al also found that the "target" composition differs from both the photosphere and the corona. These results support the idea that interplanetary events that are impulsive and have unusual compositions originate in the flare region itself, whereas gradual interplanetary particle events arise from a shock well separated from the flare.

5.11 *Microflares*

Frequent small nonthermal events offer a theoretically enticing means of releasing energy in an active plasma. Such events have been termed "microflares" or

"nanoflares." The terms refer to the calibration of one flare = 10^{33} ergs, whence "micro" and "nano" would refer to 10^{27} ergs and 10^{24} ergs total energy release per event, respectively. One could theoretically apply such a phenomenon to coronal heating in a quasi-steady state (Parker 1988) or to microscopic energy releases within a solar flare (de Jager & de Jonge 1978, Kaufmann et al 1986). Do microflares exist, and can they help with flare energy or coronal heating? The new instrumentation on *Yohkoh* and *CGRO* has made a step forward, offering new levels of sensitivity both in soft X rays (interpreted as the signature of heating) and hard X rays (interpreted as the signature of nonthermal energy release).

Although the BATSE instrument on *CGRO* has a large collecting area, it is not quite as sensitive to microflares as the solid state detectors in the pioneering observations (Biesecker et al 1994b, Lin et al 1984). However, its combination of large area and long observations allows us to make substantial progress on the hard X-ray microflare problem. If one adopts a crude relationship between the 20 keV peak flux and total flare energy, then the BATSE hard X-ray observations imply a detection limit on the order of 10^{26} ergs.

The key to establishing continuous heating through microflaring lies in the nature of the distribution of microflare total energies (Hudson 1991). In all studies thus far, including the *CGRO* observations (Biesecker et al 1994a,b; Crosby et al 1993; Schwartz et al 1992), the power-law index of the total energy distribution is flatter than the critical slope $\gamma = -2$, implying that microflares do not contribute significantly to the total energy in the corona (Collura et al 1983, Hudson 1991) (Figure 16, *bottom*). (The distribution function, analogous to the $\log N / \log S$ distribution, is given by $dN/dW \propto W^{-\gamma}$ events/unit total energy.) In a distribution this flat, the bulk of the energy is in the flares themselves, i.e. in the bright end of the distribution.

The SXT instrument on *Yohkoh* similarly has taken a major step beyond its predecessors (Schadee et al 1983). The *GOES* photometry is a convenient standard of reference, extending far backwards in time and overlapping with the photometry from the *SOLRAD* spacecraft (Horan 1971). The *GOES* photometers are relatively simple whole-Sun ionization chambers, and their sensitivity is poor—the lack of sensitivity results from source confusion, which SXT solves by imaging. Shimizu (1994) has made a statistical analysis of the SXT microflare data and again found a good match to the general power-law distribution with slope flatter than -2 (Figure 16, *top*). Thus, the X-ray microflares as observed with the sensitivity of BATSE and SXT do not seem capable of providing continuous heating for the corona.

5.12 *Identification of Fast-Drift Radio Bursts*

"Fast-drift" radio bursts (types III, V, and U) have long been known to arise in streams of nonthermal electrons with velocities on the order of $c/6$–$c/3$, thus with energies in the range of the deka-keV impulsive phase electrons. The

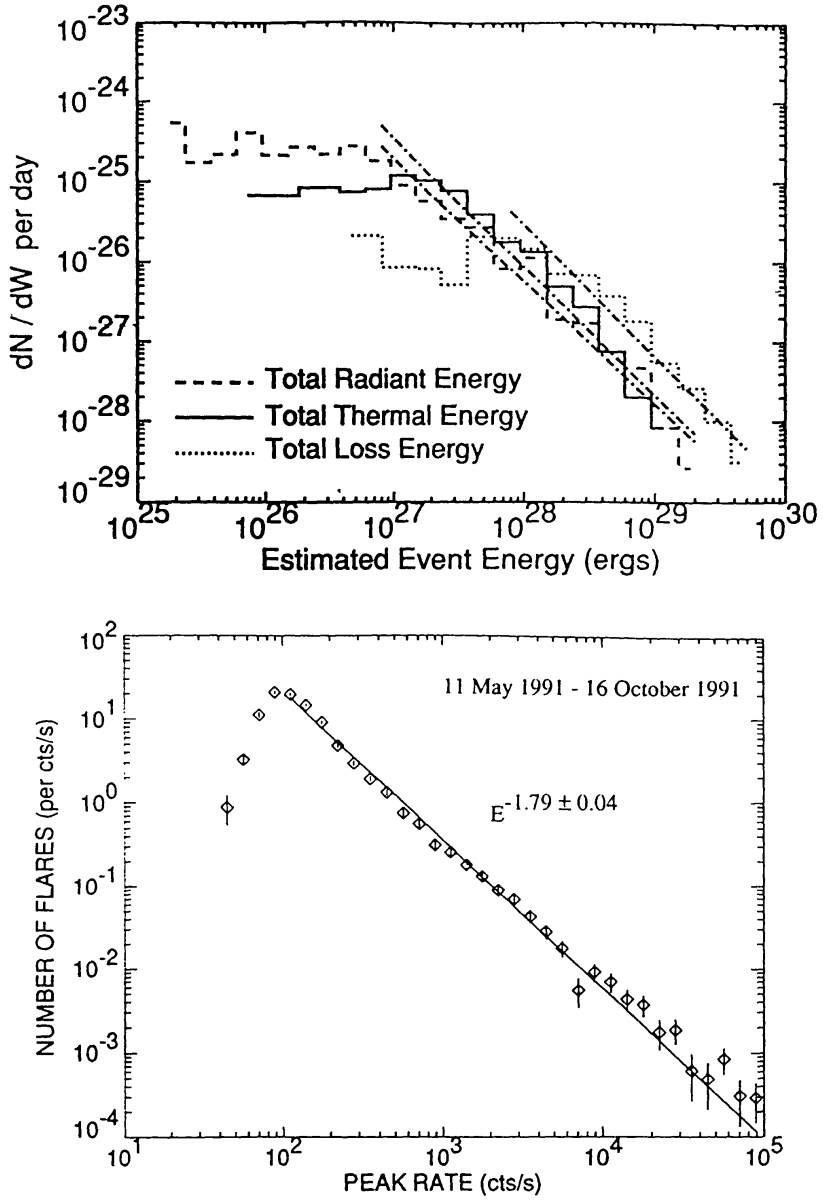

Figure 16 (*Top*) Distribution of microflares seen in soft X rays (Shimizu 1994) by *Yohkoh*/SXT, which has extended the observing range to smaller events. The different histograms show estimates of the total radiant energy, total thermal energy, and total energy loss estimated from the observed parameters. All agree on a relatively flat distribution matching that observed for more energetic events. Based upon such a flat distribution, still smaller events cannot significantly increase the total energy input. (*Bottom*) Distribution of microflares seen in hard X rays (Biesecker et al 1994a) by the large-area scintillation counters on the *Compton Gamma-Ray Observatory*. The shape of this distribution agrees well with that found for soft X rays, with the implication that nonthermal energy release continues to be comparably as important for the microflares as for the ordinary flares.

"drift" refers to the variation to lower frequency with time as the particles move through coronal plasma of decreasing density and excite plasma-frequency oscillations that couple into radiation. The solar structures (jets and large-scale coronal loops) supporting these fast-drift bursts have recently been identified by direct soft X-ray imaging compared with meter-wave dynamic spectra and source localization (Aurass et al 1994, Kundu et al 1994a, Pick et al 1994). They consist of highly collimated soft X-ray structures. Figure 17 shows a soft X-ray "jet" (Shibata et al 1992, 1994; Strong et al 1992) associated with a type III burst group observed at the Nançay radioheliograph. The X-ray jet shows us the dense channel required to explain the escape of the type III radiation. At the present time, there has been no identification of the soft X-ray structures of fast-drift bursts in ordinary flares, despite the strong statistical association of type III bursts with flares, nor (for that matter) other meter-wave phenomena associated with flares and high-energy particles in the corona (e.g. type II or type IV).

Timing observations also provide key information about the acceleration process for these microscopic processes. Aschwanden et al (1993) found a close association between repetitive decimeter bursts (type III, U, and reverse drift) and fast substructure in hard X-ray emission. The correlated patterns were found in all events brighter than a (hard X-ray) threshold level, implying that the key to their nondetection before was a poor signal-to-noise ratio resulting from low counting rates. Figure 18 illustrates the correlation. Aschwanden et al suggest that the entire impulsive-phase acceleration process can be ascribed

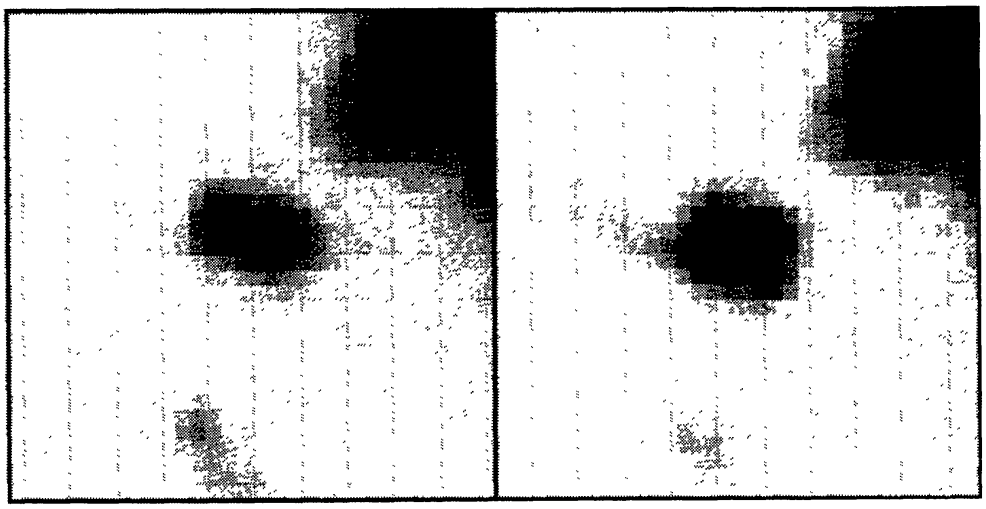

Figure 17 Soft X-ray image of a plasma jet associated with a type III radio burst (16 August 1994 13:27:28 UT; Kundu et al 1994b): (*left*) prior to the event, (*right*) 128 seconds later. The jet appears in the middle of the right image, extending to the left (East). Several different studies of *Yohkoh* and Nançay data have now identified fast-drift meter wave bursts, known to be caused by high-energy electrons, with collimated structures similar to this. The pixel size is 2.46″ for a total field of view slightly larger than 100,000 km at the Sun.

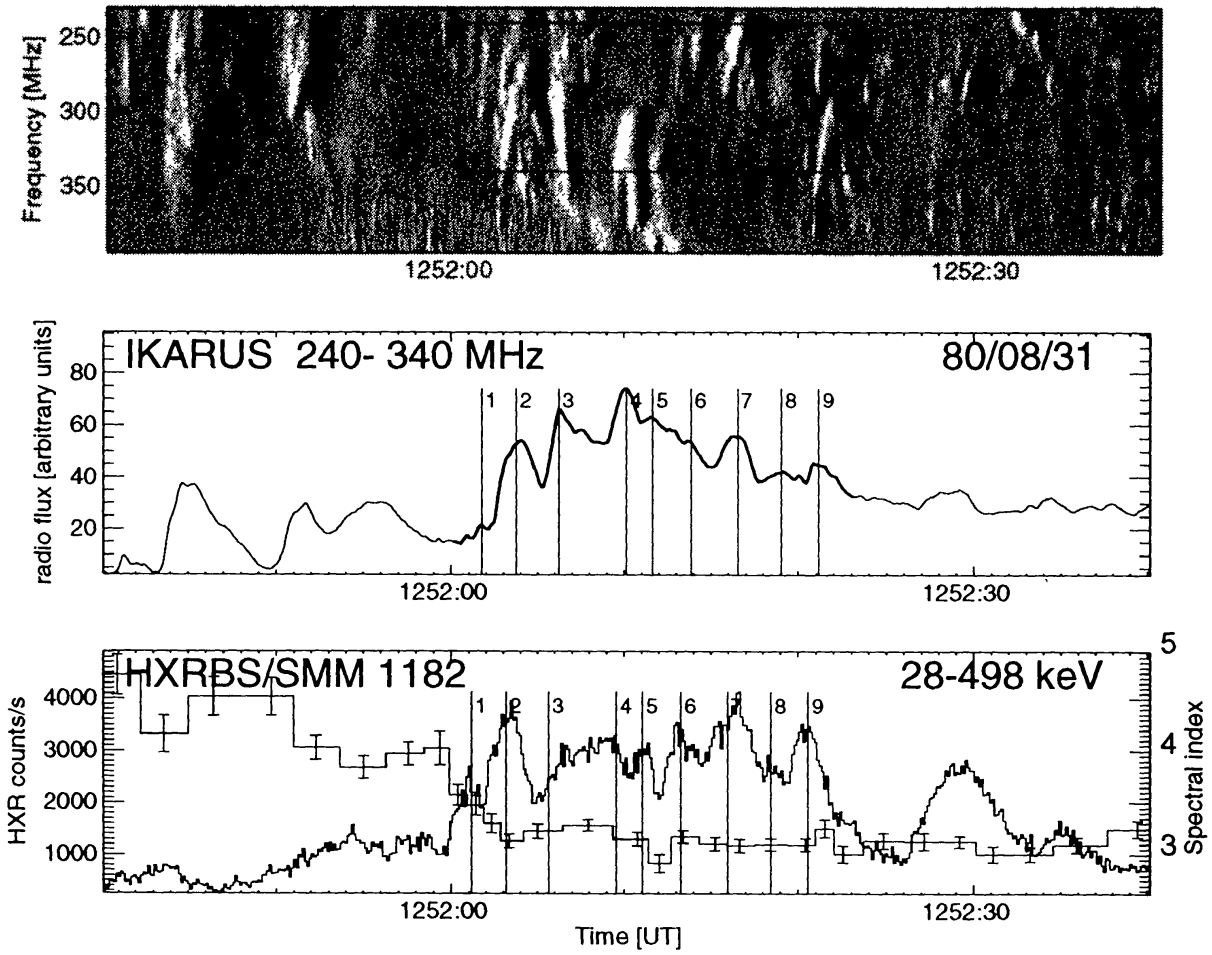

Figure 18 Correlated hard X-ray and decimeter structures (Aschwanden et al 1993). The upper panel shows an enhanced gray-scale representation of the decimeter dynamic spectrum during one minute of a flare observed jointly by the ground-based Ikarus spectrometer and by the hard X-ray instrument on the *Solar Maximum Mission*. The rapid fluctuations agree well with one another, as illustrated by the time series in the middle and lower panels.

to a superposition of many quasi-periodic acceleration episodes, each of limited energy release in a small volume.

6. DISCUSSION

6.1 *Where are the Particles?*

As mentioned in Section 1, we know of many populations of accelerated (non-thermal) particles in the solar corona, especially during flares. Radio techniques demonstrated this many years ago (Wild et al 1963) and now high-energy observations are reaching sensitivity levels good enough to be able to observe many of the same phenomena. In general, the X-ray and γ-ray observations are diagnostically easier, with fewer questions about radiative transfer or complicated

emission mechanisms that depend upon the magnetic field and its geometry. We know much more about the electrons than about the ions because of the strength of their coupling to electromagnetic radiation signatures and because of the relative ease of the observational techniques in X rays as opposed to γ rays.

The observations reviewed here establish clearly the important role of nonthermal particles in flares. We have been able to improve our ability to locate these particles within the structures (loops, jets, footpoint/ribbon regions) observed at other wavelengths and have strengthened the conclusion that such particles transport a large fraction of the energy released in a flare. The imaging observations have given us the surprising result that impulsive hard X-ray emission can also come from the corona itself, normally thought to be too collisionless to be luminous in hard X rays (but see Kane et al 1992). This and other data seem to imply the transient existence of high-density regions in unexpected parts of the corona.

The new hard X-ray imaging and timing results also point the way to the use of nonthermal particles as probes of the coronal magnetic field geometry. Direct observations of the coronal magnetic field are difficult, and extrapolations of the photospheric field are subject not only to the normal effects of error propagation in the data, but also to some theoretical uncertainty. From a theoretical point of view, particles spiraling along field lines represent the most direct method for defining the field configuration. The *Yohkoh*/HXT observation of simultaneous brightenings at paired locations establishes that the conjugate points at the opposite ends of an active flux tube can be identified in this manner. Furthermore, the radio/X-ray timing results establish that rapid variability commonly occurs (Aschwanden et al 1993). This conjugate point approach can in principle follow variations in connectivity due to reconnection and would be limited only by the resolution and sensitivity of the hard X-ray observations.

We now know that accelerated solar protons and ions exist almost everywhere. We assume that although they are always present in the immediate flare environment, many are transported to remote locations on the Sun and many escape into interplanetary space in the form of ^{3}He-rich and electron-rich particle events. They are produced remotely by shocks associated with the flare (or CME), even at large distances from the solar surface. Observations show many examples of remote brightenings clearly associated with flares occurring a considerable distance away. The γ-ray data from the 29 September 1989 event also point to long-range transport of energetic particles. In fact, the multiple loop involvement detected in the 3 June 1982 flare (Trottet et al 1994) supports this idea, complicating data interpretation that uses single-loop transport and acceleration models (e.g. Mandzhavidze & Ramaty 1992, Ryan & Lee 1991). These remote effects imply that the particles responsible for the brightenings must attain great altitudes in their transport over such great distances. This

fits in with some of the hard X-ray occultation data, dating back to Hudson (1978) and more recent work (Kane et al 1982, Kane et al 1992), showing that energetic particles, in this case electrons, exist and are even accelerated at great altitudes.

6.2 *How are the Particles Accelerated?*

Explaining the different populations of high-energy particles appears to require more than a single mechanism for their acceleration. Perhaps the best understood of these mechanisms is the shock acceleration of interplanetary ions, but it is also clear that even for the interplanetary populations more than a single mechanism is needed. Furthermore, it is not clear to what extent these interplanetary populations participate in the flare processes—most probably, not at all. There are strong indications that most of the MeV particles in space are unrelated to those producing the high-energy photon emission (Kahler 1992, Reames 1992). The prompt ground-level event (GLE) protons[3] and impulsive interplanetary particles with compositional anomalies (i.e. ^{3}He- and electron-rich) are linked more closely to the flare particle populations, such as the γ-ray producing protons. The shock wave responsible for interplanetary MeV proton acceleration often appears to have a closer relationship to the coronal mass ejection associated with the flare than to the flare itself; however, we know that there is also a large-scale wave launched at the time of the impulsive phase that has both MHD (the Moreton wave) and nonthermal (type II burst) consequences. Theoretical work suggests how compositional anomalies can arise through selective injection and acceleration (Fisk 1978, Miller & Ramaty 1992, Miller & Viñas 1993). Miller & Viñas invoke electromagnetic ion-cyclotron waves excited by electron beams as the selection and acceleration agent.

In the flare itself, we now have much knowledge of the behavior of 10–100 keV electrons, but not enough to pin down their acceleration mechanism. Because they don't radiate efficiently, we know far less about the protons in this energy range. In the extreme, it is possible that protons dominate the particle energy budget (Simnett 1986), and the behavior of the electrons would then be determined entirely by the overwhelming presence of low-energy protons. The rapid variability of the hard X-ray flux and other evidence point to multiple acceleration sites within a single event, and it seems natural to suppose that the fundamental energy release of a flare occurs in the form of discrete impulses, possibly associated with different "microscopic" elements of the flaring plasma. This could point to particle acceleration due to electric fields associated with a given reconnection event, or it could point to stochastic acceleration due to waves or nonlinear phenomena created during the turbulent conditions of the primary energy release (Vlahos 1994).

[3]These showers, produced by the highest-energy solar cosmic rays, can be detected at the surface of the Earth and provided some of the first evidence for solar particle acceleration.

The geometry of the hard X-ray emission as observed by Masuda et al (1994) strongly suggests a helmet-streamer topology with the dynamics described by the calculations of Forbes et al (1989). Producing hard X rays requires high densities in the vicinity of the reconnection site. This would also result in a harder X-ray spectrum at the footpoints due to collisional damping of the lower-energy electrons near their origin. This does not appear to be observed, nor are the high densities a part of the reconnection theory. However, one might find an explanation in a high degree of turbulence. The turbulence may be necessary to accelerate the electrons in the first place, either as the diffusing agent required by shock acceleration or as second-order Fermi acceleration. In either case the transport of the electrons is limited by the slow spatial diffusion associated with the acceleration process. The effect of the diffusive transport on the hard X-ray spectral distributions has yet to be considered theoretically. Also, the dynamic effects of the nonthermal electrons on the diffusing region need to be considered: The electrons (and protons perhaps) must be largely responsible for chromospheric evaporation, as discussed above.

The acceleration process for protons is only somewhat clearer. In interplanetary space there are good indications that shocks accelerate protons in a majority of events. With the current data from the time-extended high-energy γ-ray flares there is growing evidence that a single acceleration episode cannot explain the hard proton spectrum responsible for γ rays with $E > 50$ MeV (Forrest et al 1986, Ramaty & Mandzhavidze 1994), thereby lending support for a prolonged and continuous acceleration process. This prolonged acceleration most likely takes the form of second-order stochastic Fermi acceleration (Ryan et al 1994b, Ryan & Lee 1991) because the emission can be so protracted that any coronal shock must be far removed from the Sun. The acceleration volume must therefore be large (MacKinnon 1991) and thus points toward trapping in large loops, similar to the requirements for some kinds of meter-wave bursts. Passive trapping of previously accelerated protons from the impulsive phase is difficult on several counts (Smith & Brecht 1986). The first problem is the extremely low value of the upper limit for MHD turbulence within a coronal loop. An 8-hour trapping time, where the trapping is similar to that in the Earth's radiation belts, implies that the scattering mean free path of an energetic proton be on the order of 10^4 solar radii. The common existence of turbulence in the corona as evidenced in radio wave scattering (Bastian 1994), for example, makes such calm environments unlikely. For shorter trapping times in smaller loops, particle drifts (curvature and gradient) become a problem that can only be alleviated by requiring unusual loop geometries with twists in the magnetic field approaching the theoretical maximum before the loops buckle (Lau et al 1993, Lau & Ramaty 1994). [Passive trapping with some degree of pitch-angle scattering will in many flares modify the precipitation rate of energetic particles, consequently modifying the hard X-ray and γ-ray intensity-time profiles

(e.g. Ramaty et al 1990, Ryan 1986).] It is simpler to assume that the prolonged turbulence in loops, or perhaps an ensemble of shocks imbedded in a loop (Anastasiadis & Vlahos 1994), not only causes the diffusive transport of protons, but accelerates them as well. Long-duration trapping and acceleration follow from large-scale structures, where for a given level of turbulence the residence time is related directly to the loop size. The widespread γ-ray emission from the flare of 29 September 1989 provides support for this idea that large volumes of the solar corona can be involved in the more pronounced high-energy events. There is also ample evidence that sufficient energy exists within the loops for them to maintain high temperatures (and MHD turbulence) for long periods of time (Jakimiec et al 1986).

The origin of the impulsive phase ion acceleration, however, remains unclear (Smith & Brecht 1988). It is difficult to rule out shock acceleration, second-order Fermi acceleration, or dc electric fields. Arguments based on spectra should be taken cautiously. During the impulsive phase all three of these processes will produce non-power-law spectra (e.g. Achterberg & Norman 1980, Lee 1994, Lee & Ryan 1986). Historically, proton momentum spectra deduced from γ-ray data have been described in terms of a Bessel function with a hardness parameter αT (e.g. Murphy & Ramaty 1984, Ramaty 1986). This description dates back to second-order Fermi leaky box calculations (Fermi 1949, Forman et al 1986, Lee 1994, Parker 1957, Schlickeiser 1989), where α is the "acceleration efficiency" and T is the escape time from the leaky box. This description enjoys success primarily because it (*a*) does not diverge at low energies and (*b*) has an exponential cutoff at the high end, but the model itself, with a single escape time, must be too simple. Shock acceleration, on the other hand, will also produce a high-energy cutoff because the limited time for acceleration and the limited size of the shock. Electric fields have, of course, a high-energy cutoff at the value of the maximum potential drop. The subsequent convolution of the various proton spectra into γ-ray spectra is subject to all the detailed conditions of the geometry, plasma environment, and the particle composition of the ions and the solar corona. No firm experimental evidence exists to discriminate among these candidate acceleration processes.

Theoretical work is being conducted on all these acceleration scenarios, primarily for the problem of the impulsive-phase electrons, which is the most challenging (Melrose 1994). Electron acceleration tends to be the more difficult to address, because the electrons interact with a greater variety of dispersive plasma waves and the cyclotron radii are so small, making them sensitive to the small-scale structure in shock fronts. The electron acceleration process itself produces departures from a pure power-law spectrum (Petrosian 1994). Neither opacity nor transport effects can explain the break at high energies in the high-energy γ-ray spectrum of electron-rich flares, although synchrotron

losses under the right conditions may turn the spectrum over at high energies. Transport effects do, however, produce an increased bremsstrahlung luminosity (limb brightening) at the solar limb (Dermer 1987, Miller & Ramaty 1989, Petrosian 1985), which has been difficult to observe (e.g. Bogovalov et al 1985, Kane et al 1988, Vestrand et al 1987). There are several problems that plague second-order Fermi acceleration theory for electrons: the correct selection of wave modes that provide the scattering, the intense level of turbulence required, and the depletion of the turbulence energy by the exciting electrons and/or ions (Miller & Steinacker 1992). LaRosa et al (1994) use the turbulence associated with the magnetic reconnection process to accelerate nonthermal electrons in the impulsive phase. Many of the same problems afflict acceleration of electrons with coronal shocks. Electric field models, on the other hand, usually suffer the problems of accelerating all the electrons to low energies, inefficiency at high energy, and requiring a return current to balance the current of the mobile electrons (Holman 1985).

The particle acceleration problem of electron-rich γ-ray flares is perhaps the most challenging. Few attempts have been made to address this problem. The paucity of nuclear lines in these events suggests that some unusual condition prevails for the preferential acceleration of electrons to high energies, e.g. runaway DC electric field acceleration. Such a situation can arise from a neutral beam (Speiser 1965) of sufficient flux density impacting the chromosphere (Simnett 1991). With the beam electrons being scattered in the dense chromosphere, the momentum of the beam protons sets up a DC field accelerating the scattered electrons up to the potential voltage. This model would imply that a minimum intensity exists for electron-rich γ-ray flares. Such a threshold has not been reported.

6.3 *How do Flares Work?*

Thanks to the recent data, we are quite sure now that magnetic reconnection accompanies many, if not all, flares. By magnetic reconnection, we mean here a geometrically noticeable change in the connectivity of the magnetic field lines participating in the flare.[4] The strongest evidence comes from the cusp or helmet-streamer configuration (Figure 15) establishing the presence of a neutral sheet in the corona above the flare. The actual reconnection process, and the plasma flows that it requires, have been surprisingly difficult to confirm unambiguously, and the reconnection theory does not appear to have much predictive power. Nevertheless, it is well known that type III bursts and sprays seen in Hα frequently occur at the impulsive phase of a flare, and this has now been confirmed at high energies by the *Yohkoh* soft X-ray observations of flare

[4]This kind of reconnection, either in a helmet-streamer or emerging-flux geometry, changes the topology of the magnetic field. Alternatively, an energy release internal to a loop (Alfvén & Carlqvist 1967) does not appear to involve new topology but can also be described as a reconnection process.

ejecta. These ejecta may be the expected reconnection jets. The key question remains open, however: Does the reconnection that we are now beginning to see quite clearly really provide the flare energy from a coronal reservoir? The answer is probably yes, but quantitative proof is currently lacking, and the possibility remains open that the energy production in the impulsive phase really comes from reconnection events on small scales—internal to the magnetic loops themselves—rather than the larger scales that are easier to observe. However, drawing a distinction between these two alternatives may be splitting hairs from the point of view of the energetic particles, which are only described inadequately by present theories.

The observational uncertainty about the causes and effects of small-scale structure—turbulence—appears frequently in discussions of high-energy particles in solar flares and their observational consequences. Microscopic motions might play a role in spectroscopic line broadening, particle acceleration, image distortion at radio wavelengths, structure definition in interplanetary scintillation, plasma emissivity, magnetic reconnection and energy release in magnetic neutral sheets, etc. Nonetheless, few reliable tools for direct observation of wave amplitudes currently exist. This seems to be one of the most important gaps in our knowledge of the physics of high-energy particles in solar flares and in the more general question of how flares work.

Finally, the concept of "self-organized criticality" has been applied to the problems of solar flares by Lu & Hamilton (1991) and Lu et al (1993). It offers some explanations, for example, a model-independent derivation of the observed power-law distribution of flare occurrence.

7. CONCLUSIONS

In this review we have discussed mainly the data from the new high-energy observatories operating in space during the maximum solar activity of Cycle 22. As has been known for a long time, particle acceleration has an inseparable relationship with many of the phenomena of the active Sun. This is fortunate, because we can use the particles as probes of the fundamental nonthermal properties of flares and other forms of solar magnetic activity. The past decade has been a fruitful time because of the new generation of observing instruments. As usual, though, the data have not resolved some of the most important issues and only point the way towards real understanding. We offer here some questions that should be addressed by future observations:

1. Can hard X-ray timing and imaging establish the geometry of the reconnection that causes the flare energy release?

2. Do the energetic particles seen in the interplanetary medium ever "escape" from the flare structures themselves, or are they accelerated remotely?

3. Do the deka-keV electrons of the impulsive phase have a monoenergetic distribution (electric field) or a distributed energy profile (stochastic process)?

4. Are the pion-producing ions stored in the corona, or does acceleration continue for hours in a major flare?

5. How is the shock wave responsible for coronal particle acceleration originally created?

6. Do coronal mass ejections and flare events arise from similar physical mechanisms?

7. What are the coronal structures (as observed in soft X rays) that produce the meter-wave events associated with flares (e.g. type II and type IV)?

8. Can we develop observational tools that will help us to establish the turbulent state of the flaring plasma?

ACKNOWLEDGMENTS

We thank the following persons for helpful commentary and discussion of early versions of this review: D Alexander, T Forbes, S Kahler, M Lee, and T Sakao. We also thank Ms. Naomi Preble for her assistance in preparing this manuscript. The work of Hudson was supported by NASA under contract NAS 8-37334. The work of Ryan was supported by NASA under contract NAS5-26645.

Literature Cited

Achterburg A, Norman CA. 1980. *Astron. Astrophys.* 89:353–62
Acton L, Tsuneta S, Ogawara Y, Bentley R, Bruner M, et al. 1992a. *Science* 258:618–25
Acton LW, Canfield RC, Gunkler TA, Hudson HS, Kiplinger AL, Leibacher JW. 1982. *Ap. J.* 263:409–22
Acton LW, Feldman U, Bruner ME, Doschek GA, Hirayama T, et al. 1992b. *Publ. Astron. Soc. Jpn.* 44:L71–75
Akimov VV, Afanassyev VG, Belaousov AS, Blokhintsev ID, Kalinkin LF, et al. 1991. *22nd Int. Cosmic Ray Conf., Dublin, Ireland,* 3:73–76
Akimov VV, Belov AV, Chertok IM, Kurt VG, Leikov NG, et al. 1994. See Enome & Hirayama 1994, pp. 371–74
Alexander D, Dunphy PP, MacKinnon AL. 1994. *Sol. Phys.* 151:147–67
Alfvén H, Carlqvist P. 1967. *Sol. Phys.* 1:220–28
Anastasiadis A, Vlahos L. 1994. *Ap. J.* 428:819–26
Antonucci E, Dodero MA, Martin R, Peres G, Reale F, Serio S. 1993. *Ap. J.* 413:786–97
Aschwanden M, Benz AO, Schwartz RA. 1993. *Ap. J.* 417:790–804
Aschwanden MJ, Montello ML, Dennis BR, Benz AO. 1995. *Ap. J.* 440:394–406
Aurass H, Klein K-L, Martens P. 1994. *Sol. Phys.* 155:203–6
Bai T, Ramaty R. 1978. *Ap. J.* 219:705–26
Bai T, Sturrock PA. 1989. *Annu. Rev. Astron. Astrophys.* 27:421–67
Barat C, Trottet G, Vilmer N, Dezalay JP, Talon R, et al. 1994. *Ap. J. Lett.* L109–12
Bastian TS. 1994. *Ap. J.* 426:774–81
Benka SG, Holman GD. 1992. *Ap. J.* 391:854–64

Bentley RD, Doschek GA, Simnett GM, Rilee ML, Mariska JT, et al. 1994. *Ap. J.* 421:L55–58
Biesecker D, Ryan JM, Fishman GJ. 1994a. See Ryan & Vestrand 1994, pp. 83–86
Biesecker DA, Ryan JM, Fishman GJ. 1994b. In *Advances in Solar Physics, Catania, Italy,* ed. G Belvedere, M Rodonò, GM Simnett, 432:225–30. Berlin: Springer-Verlag. 335 pp.
Bogovalov SV, Kotov YD, Zenchenko VM, Vedrenne G, Niel M, et al. 1985. *Sov. Astron. Lett.* 11:322–24
Boldt E, Serlemitsos P. 1969. *Ap. J.* 157:557–62
Brosius JW, Robinson RD, Maran SP. 1995. *Ap. J. Lett.* L109–12
Brown JC. 1971. *Sol. Phys.* 18:489–502
Brown JC, Karlicky M, MacKinnon AL, van den Oord GHJ. 1990. *Ap. J. Suppl.* 73:343–48
Brueckner GE, Bartoe J-DF. 1993. *Ap. J.* 272:329–48
Cane HV, McGuire RE, von Rosenvinge TT. 1986. *Ap. J.* 301:448–59
Canfield RC, Chang C-R. 1985. *Ap. J.* 295:275–84
Canfield RC, Cook JW. 1978. *Ap. J.* 225:650–54
Carmichael H. 1964. *AAS-NASA Symp. on the Physics of Solar Flares, Greenbelt, MD,* ed. WN Hess, pp. 451–56. *NASA SP-50*
Carrington RC. 1859. *MNRAS* 20:13–15
Cheng C-C, Rilee M, Uchida Y. 1994. See Enome & Hirayama 1994, pp. 213–16
Chupp EL. 1984. *Annu. Rev. Astron. Astrophys.* 22:359–87
Chupp EL. 1990. *Ap. J. Suppl.* 73:213–26
Chupp EL, Debrunner H, Flückiger E, Forrest DJ, Golliez F, et al. 1987. *Ap. J.* 318:913–25
Chupp EL, Forrest DJ, Higbie PR, Suri AN, Tsai C, Dunphy PP. 1973. *Nature* 241:333–35
Chupp EL, Forrest DJ, Ryan JM, Heslin J, Reppin C, et al. 1982. *Ap. J.* 263:L95–99
Chupp EL, Forrest DJ, Vestrand WT, Debrunner H, Flückiger E, et al. 1985. *19th Int. Cosmic Ray Conf., La Jolla, CA,* 4:126–29
Cliver EW, Dennis BR, Kiplinger AL, Kane SR, Neidig DF, et al. 1986. *Ap. J.* 305:920–35
Collura A, Pasquini L, Schmitt JHMM. 1983. *Astron. Astrophys.* 203:197–206
Cornell ME, Hurford GJ, Kiplinger AL, Dennis BR. 1984. *Ap. J.* 279:875–881
Crosby NB, Aschwanden MJ, Dennis BR. 1993. *Sol. Phys.* 143:275–99
Culhane JL, Phillips AT, Kosugi T, Inda-Koide M, Pike CD. 1994. See Enome & Hirayama 1994, pp. 117–21
de Jager C, de Jonge G. 1978. *Sol. Phys.* 58:127–37
Debrunner H. 1994. See Ryan & Vestrand 1994, pp. 207–21
Debrunner H, Flückiger E, Chupp EL, Forrest DJ. 1983. *18th Int. Cosmic Ray Conf., Bangalore,* 4:75–78
Debrunner H, Flückiger EO, Lockwood JA. 1990. *Ap. J. Suppl.* 73:259–62
Debrunner H, Lockwood JA, Ryan JM. 1993a. *Ap. J.* 409:822–29
Debrunner H, Lockwood JA, Ryan JM, McConnell M, Schönfelder V, et al. 1993b. *23rd Int. Cosmic Ray Conf., Calgary, Alberta,* 3:115–18
Dennis BR, Zarro D. 1993. *Sol. Phys.* 146:177–90
Dermer CD. 1987. *Ap. J.* 323:795–98
Dingus BL, Sreekumar P, Bertsch DL, Fichtel CE, Hartman RC, et al. 1994. See Ryan & Vestrand 1994, pp. 177–79
Duijveman A, Hoyng P, Machado ME. 1982. *Sol. Phys.* 81:137–57
Dulk GA. 1985. *Annu. Rev. Astron. Astrophys.* 23:169–24
Dunphy PP, Chupp EL. 1994. See Ryan & Vestrand 1994, pp. 112–17
Emslie AG, Brown JC. 1985. *Ap. J.* 295:648–53
Enome S, Hirayama T, eds. 1994. *Proc. Kofu Symp., Kofu, NRO Rep. 360.* Nobeyama: Nobeyama Radio Obs.
Evenson P, Kroeger R, Meyer P, Reames D. 1990. *Ap. J. Suppl.* 73:273–77
Evenson P, Meyer P, Pyle KR. 1983. *Ap. J.* 274:875–82
Feldman U, Seely JF, Doschek GA, Strong KT, Acton LW, et al. 1994. *Ap. J.* 424:444–58
Fermi E. 1949. *Phys. Rev.* 75:1169–74
Fishman GJ, Meegan CA, Wilson RB, Paciesas WS, Parnell TA, et al. 1989. *Proc. Gamma Ray Obs. Sci. Workshop, Goddard Space Flight Center, Greenbelt, MD,* ed. WN Johnson, 2.39–2.50. Greenbelt, MD: NASA
Fisk LA. 1978. *Ap. J.* 224:1048
Fleishman GD, Kahler SW. 1992. *Ap. J.* 394:688–96
Forbes TG, Malherbe JM, Priest ER. 1989. *Sol. Phys.* 120:285–307
Forman MA, Ramaty R, Zweibel EG. 1986. In *The Physics of the Sun,* ed. PA Sturrock, TE Holzer, DM Mihalas, RK Ulrich, II:249–89. Dordrecht: Reidel. 385 pp.
Forrest DJ, Chupp EL. 1983. *Nature* 305:291–92
Forrest DJ, Chupp EL, Ryan JM, Cherry ML, Gleske IU, et al. 1980. *Sol. Phys.* 65:15–23
Forrest DJ, Vestrand WT, Chupp EL, Rieger E, Cooper J. 1986. *Adv. Space Res.* 6:115–18
Forrest DJ, Vestrand WT, Chupp EL, Rieger E, Cooper J, Share G. 1985. *19th Int. Cosmic Ray Conf., La Jolla, CA,* 4:146–49
Gary DE. 1985. *Ap. J.* 297:799–804
Gehrels N, Chipman E, Kniffen DA. 1993. In *Compton Symp., Washington Univ., St. Louis,* ed. M Friedlander, N Gehrels, D Macomb, 280:3–17. New York: Am. Inst. Phys. 1230 pp.
Gehrels N, Chipman E, Kniffen DA. 1994. *The Second Compton Symp., College Park, MD,* ed. CE Fichtel, N Gehrels, JP Norris, 304:3–

11. New York: Am. Inst. Phys. 786 pp.
Gosling JT. 1993. *J. Geophys. Res.* 98:18,937–49
Hachenberg O, Wallis G. 1961. *Z. Astrophys.* 52:42–72
Haisch B, Strong KT, Rodonò M. 1991. *Annu. Rev. Astron. Astrophys.* 29:275–24
Hanaoka Y, Kurokawa H, Saito S. 1986. *Sol. Phys.* 105:133–48
Harvey KL, Sheeley NR, Harvey JW. 1986. *Solar-Terrestrial Predictions: Proc. of a Workshop at Meudon, France, June 18–22, 1984, Meudon, France,* ed. PA Simon, G Heckman, MA Shea, pp. 198–203. Boulder: Natl. Ocean. Atmos. Admin.
Henoux JC, Aboudarham J, Brown JC, Van Den Oord GHJ, Van Driel-Gesztelyi L. 1990a. *Astron. Astrophys.* 233:577–82
Henoux JC, Chambe G, Feautrier N, Smith D, Tamres D. 1990b. *Ap. J. Suppl.* 73:303–11
Heristchi D. 1986. *Ap. J.* 311:474–84
Hirayama T. 1974. *Sol. Phys.* 34:323–38
Holman GD. 1985. *Ap. J.* 293:584–94
Horan DM. 1971. *Sol. Phys.* 21:188–97
Hoyng P, Duijveman A, Machado ME, Rust DM, Svestka Z, et al. 1981. *Ap. J. Lett.* 246:L155–59
Hua X-M, Lingenfelter RE. 1987. *Sol. Phys.* 107:351–83
Hudson H. 1994. See Ryan & Vestrand 1994, pp. 151–61
Hudson HS. 1972. *Sol. Phys.* 24:414–28
Hudson HS. 1973. In *High Energy Phenomena on the Sun, Greenbelt, MD,* ed. R Ramaty, RG Stone, pp. 207–20. *NASA SP-342*
Hudson HS. 1978. *Ap. J.* 224:235–40
Hudson HS. 1991. *Sol. Phys.* 133:357–69
Hudson HS, Acton L, Hirayama T, Uchida Y. 1992. *Publ. Astron. Soc. Jpn.* 44:L77–81
Hudson HS, Acton LW, Sterling AC, Tsuneta S, Fishman J, et al. 1994a. *Proc. Int. Symp. on the Yohkoh Scientfic Results, Sagamibara, Kanagawa,* ed. Y Uchida, T Watanabe, K Shibata, HS Hudson, pp. 143–45. Tokyo: Universal Acad. Press
Hudson HS, Canfield RC, Kane SR. 1978. *Sol. Phys.* 60:137–42
Hudson HS, Driel-Gesztelyi LV, Kosugi T. 1994b. See Enome & Hirayama 1994, pp. 397–400
Hudson H, Haisch B, Strong KT. 1995. *J. Geophys. Res.* 100:3473–77
Hudson HS, Strong KT, Dennis BR, Zarro D, Inda M, et al. 1994c. *Ap. J. Lett.* 422:L25–27
Jakimiec J, Sylwester B, Sylwester J, Lemen JR, Mewe R, et al. 1986. *Solar Maximum Analysis: Proc. Int. Workshop, 17–24 June, 1985, Irkutsk, USSR,* ed. VE Stepanov, VN Obridko, pp. 91–101. Utrecht: VNU Sci.
Johnson WN, Kinzer RL, Kurfess JD, Strickman MS, Purcell WR, et al. 1993. *Ap. J. Suppl.* 86:693–712
Kahler SW. 1992. *Annu. Rev. Astron. Astrophys.* 30:113–41
Kanbach G, Bertsch DL, Fichtel CE, Hartman RC, Hunter SD, et al. 1993. *Astron. Astrophys. Suppl.* 97:349–53
Kane SR. 1969. *Ap. J.* 157:L139–42
Kane SR, Fenimore EE, Klebesadel RW, Laros JG. 1982. *Ap. J.* 254:L53–57
Kane SR, Fenimore EE, Klebesadel RW, Laros JG. 1988. *Ap. J.* 326:1017–31
Kane SR, McTiernan J, Loran J, Fenimore EE, Klebesadel RW, Laros JG. 1992. *Ap. J.* 390:687–702
Kaufmann P, Correia E, Costa JER, Zodi Vaz AM. 1986. *Astron. Astrophys.* 157:11–18
Kniffen D. 1989a. *Proc. Gamma Ray Obs. Sci. Workshop, Goodard Space Flight Center, Greenbelt, MD,* ed. WN Johnson, pp. 1–10. Greenbelt, MD: NASA
Kniffen DA. 1989b. *Max '91 Workshop #2: Developments in Observations and Theory for Solar Cycle 22, Laurel, MD,* ed. RM Winglee, BR Dennis, pp. 33–45
Koch HW, Motz JW. 1959. *Rev. Mod. Phys.* 31:920–55
Kocharov LG, Lee JE, Zirin H. 1994. *Sol. Phys.* 155:149–70
Kopp RA, Pneuman GW. 1976. *Sol. Phys.* 50:85–98
Kosugi T. 1994. See Enome & Hirayama 1994, pp. 11–18
Kundu MR. 1965. *Solar Radio Astronomy.* New York: Intersci. 660 pp.
Kundu MR, Shibasaki K, Enome S, Nitta N. 1994a. See Enome & Hirayama 1994, pp. 79–82
Kundu MR, Strong KT, Pick M, White SM, Hudson HS, et al. 1994b. *Ap. J. Lett.* 427:L59–62
LaRosa TN, Moore RL, Shore SN. 1994. *Ap. J.* 425:856–60
Lau Y-T, Northrop TG, Finn JM. 1993. *Ap. J.* 414:908–15
Lau Y-T, Ramaty R. 1994. See Ryan & Vestrand 1994, pp. 71–73
Lee MA. 1994. See Ryan & Vestrand 1994, pp. 134–42
Lee MA, Ryan JM. 1986. *Ap. J.* 303:829–42
Li P. 1994. *Ap. J.* 421:381–89
Lin RP, Hudson HS. 1976. *Sol. Phys.* 50:153–78
Lin RP, Schwartz RA, Kane SR, Pelling RM, Hurley KC. 1984. *Ap. J.* 283:421–25
Lin RP, Schwartz RA, Pelling RM, Hurley KC. 1981. *Ap. J. Lett.* 251:L109–14
Lu ET, Hamilton RJ. 1991. *Ap. J. Lett.* 380:L89–92
Lu ET, Hamilton RJ, McTiernan JM, Bromund KR. 1993. *Ap. J.* 412:841–52
Lu ET, Petrosian V. 1989. *Ap. J.* 338:1122–30
MacKinnon AL. 1991. *Vistas Astron.* 34:331–42
Mandzhavidze N, Ramaty R. 1992. *Ap. J.* 389:739–55
Marschhäuser H, Rieger E, Kanbach G. 1994. See Ryan & Vestrand 1994, pp. 171–76

Masuda S. 1994. *Hard X-ray sources and the primary energy release site in solar flares.* PhD thesis. Univ. Tokyo. 131 pp.
Masuda S, Kosugi T, Hara H, Tsuneta S, Ogawara Y. 1994. *Nature* 371:495–97
McConnell M. 1994. See Ryan & Vestrand 1994, pp. 21–25
McConnell M, Bennett K, Bloemen H, de Boer H, Busetta M, et al. 1993. *Adv. Space Res.* 13:245–48
McTiernan JM, Kane SR, Hurley K, Laros JG, Fenimore EE, et al. 1994. See Enome & Hirayama 1994, pp. 389–92
McTiernan JM, Kane SR, Loran JM, Lemen JR, Acton LW, et al. 1993. *Ap. J. Lett.* 416:L91–93
Meadows AJ. 1970. *Early Solar Physics.* Pergamon: New York. 312 pp.
Melrose DB. 1994. *Ap. J. Suppl.* 90:623–30
Metcalf T, Mickey D, Canfield R, Wülser J-P. 1994. See Ryan & Vestrand 1994, pp. 59–65
Miller JA, Ramaty R. 1989. *Ap. J.* 344:973–90
Miller JA, Ramaty R. 1992. *Particle Acceleration in Cosmic Plasmas, Newark, DE,* ed. GP Zank, TK Gaisser, 264:223–28. New York: Am. Inst. Phys. 498 pp.
Miller JA, Steinacker J. 1992. *Ap. J.* 399:284–93
Miller JA, Viñas A. 1993. *Ap. J.* 412:386–400
Muraki Y, Murakami K, Miyazaki M, Mitsui K, Shibata S, et al. 1992. *Ap. J. Lett.* 400:L75–78
Muraki Y, Sakakibara S, Shibata S, Murakami K, Takahashi K, et al. 1994. See Enome & Hirayama 1994, pp. 267–70
Murphy R, Share GH, Grove JE, Johnson WN, Kinzer RL, et al. 1994. See Ryan & Vestrand 1994, pp. 15–20
Murphy RJ, Dermer CD, Ramaty R. 1987. *Ap. J. Suppl.* 63:721–48
Murphy RJ, Ramaty R. 1984. *Adv. Space Res.* 4:127–36
Murphy RJ, Ramaty R, Kozlovsky B, Reames DV. 1991. *Ap. J.* 371:793–803
Murphy RJ, Share GH, Forrest DJ, Grabelsky DA, Grove JE, et al. 1993. *23rd Int. Cosmic Ray Conf., Calgary, Alberta,* 3:99–102
Murphy RJ, Share GH, Letaw JR, Forrest DJ. 1990. *Ap. J.* 358:298–312
Neidig DF, Kane SR. 1993. *Sol. Phys.* 143:201–4
Neupert WM. 1968. *Ap. J. Lett.* 153:L59–64
Nitta N, Kiplinger AL, Kai K. 1989. *Ap. J.* 337:1003–16
Ogawara Y, Takano T, Kato T, Kosugi T, Tsuneta S, et al. 1991. *Sol. Phys.* 136:1–16
Orrall FQ, Zirker JB. 1976. *Ap. J.* 208:618–32
Parker EN. 1957. *Phys. Rev.* 107:830–36
Parker EN. 1988. *Ap. J.* 330:474–79
Pelaez F, Mandrou P, Niel M, Mena B, Vilmer N, et al. 1992. *Sol. Phys.* 140:121–38
Peterson LE, Winckler JR. 1959. *J. Geophys. Res.* 64:697–707
Petrosian V. 1985. *Ap. J.* 299:987–93
Petrosian V. 1994. See Ryan & Vestrand 1994, pp. 162–70
Pick M, Raoult A, Trottet G, Vilmer N, Strong K, Magalhaes A. 1994. See Enome & Hirayama 1994, pp. 263–66
Ramaty R. 1986. In *Physics of the Sun,* ed. PA Sturrock, DM Mihalas, RK Ulrich, pp. 291–323. Dordrecht: Reidel
Ramaty R, Kozlovsky B, Lingenfelter RE. 1979. *Ap. J. Suppl.* 40:487–526
Ramaty R, Mandzhavidze N. 1994. See Enome & Hirayama, pp. 275–78
Ramaty R, Mandzhavidze N, Kozlovsky B, Skibo JG. 1993. *Adv. Space Res.* 13(9):275–84
Ramaty R, Miller JA, Hua X-M, Lingenfelter RE. 1990. *Ap. J. Suppl.* 73:199–207
Rank G, Diehl R, Lichti GG, Schönfelder V, Varendorff M, et al. 1994. See Ryan & Vestrand 1994, pp. 100–5
Reames DV. 1992. *Particle Acceleration in Cosmic Plasmas, Newark, DE,* ed. GP Zank, TK Gaisser, 264:213–22. New York: Am. Inst. Phys. 498 pp.
Reames DV, Meyer JP, von Rosenvinge TT. 1994. *Ap. J. Suppl.* 90:649–67
Rieger E. 1994. *Ap. J. Suppl.* 90:645–48
Rieger E, Marschhäuser H. 1990. *Max '91 Workshop #3, Estes Park, CO,* ed. R Winglee, A Kiplinger, pp. 68–76
Rosner R, Tucker WH, Vaiana GS. 1978. *Ap. J.* 220:643–65
Ryan J, Forrest D, Lockwood J, Loomis M, McConnell M, et al. 1993. *Compton Gamma-Ray Observatory, St. Louis, MO,* ed. M Friedlander, N Gehrels, D Macomb, 280:631–42. New York: Am. Inst. Phys. 1230 pp.
Ryan J, Forrest D, Lockwood J, Loomis M, McConnell M, et al. 1994a. See Ryan & Vestrand 1994, pp. 89–93
Ryan JM. 1986. *Sol. Phys.* 105:365–82
Ryan JM. 1994. *Second Compton Symp., College Park, MD,* ed. CE Fichtel, N Gehrels, JP Norris, 304:12–21. New York: Am. Inst. Phys. 786 pp.
Ryan JM, Aarts H, Bennett K, Byrd R, de Vries C, et al. 1992. *Data Analysis in Astronomy,* ed. VD Gesú, pp. 261–70. New York: Plenum. 364 pp.
Ryan JM, Bennett E, Lee MA. 1994b. *Advances in Solar Physics, Catania, Italy,* ed. G Belvedere, M Rodonò, GM Simnett, 432:273–78. Berlin: Springer-Verlag. 335 pp.
Ryan JM, Chupp EL, Forrest DJ, Matz SM, Rieger E, et al. 1983. *Ap. J. Lett.* 272:L61–65
Ryan JM, Lee MA. 1991. *Ap. J.* 368:316–24
Ryan JM, Vestrand WT, eds. 1994. *High-Energy Solar Phenomena—A New Era of Spacecraft Measurements, Waterville Valley, NH,* Vol. 294. New York: Am. Inst. Phys. 246 pp.
Sakao T. 1994. *Characteristics of solar flare*

hard X-ray sources as revealed with the hard X-ray telescope aboard the Yohkoh satellite. PhD thesis. Univ. Tokyo. 214 pp.
Sakao T, Kosugi T, Masuda S, Inda M, Makishima K, et al. 1992. *Publ. Astron. Soc. Jpn.* 44:L83–87
Sakao T, Kosugi T, Masuda S, Yaji K, Inda-Koide M, Makishima K. 1994. See Enome & Hirayama 1994, pp. 169–72
Schadee A, de Jager C, Svestka Z. 1983. *Sol. Phys.* 89:287–305
Schlickeiser R. 1989. *Ap. J.* 336:243–63
Schneid EJ, Brazier KTS, Kanbach G, von Montigny C, Mayer-Hasselwander HA, et al. 1994. See Ryan & Vestrand 1994, pp. 94–99
Schönfelder V, Aarts H, Bennett K, deBoer H, Clear J, et al. 1993. *Ap. J. Suppl.* 86:657–92
Schwartz RA, Dennis BR, Fishman GJ, Meegan CA, Wilson RB, Paciesas WS. 1992. *The Compton Obs. Sci. Workshop, Annapolis, MD,* ed. CR Shrader, N Gehrels, B Dennis, pp. 457–68. *NASA SP-3137*
Shea MA, Smart DF. 1991. *Geophys. Res. Lett.* 18:1655–58
Shibata K, Ishido Y, Acton LW, Strong KT, Hirayama T, et al. 1992. *Publ. Astron. Soc. Jpn.* 44:L173–79
Shibata K, Nitta N, Strong KT, Matsumoto R, Yokoyama T, et al. 1994. *Ap. J. Lett.* 431:L51–53
Shibata S. 1994. *J. Geophys. Res.* 99:6651–65
Shimizu T. 1994. See Enome & Hirayama 1994, pp. 61–64
Simnett G. 1986. *Sol. Phys.* 106:165–83
Simnett G. 1991. *Philos. Trans. R. Soc. London Ser. A* 336:439–50
Smith DF, Brecht SH. 1986. *Ap. J.* 306:317–22
Smith DF, Brecht SH. 1988. *Sol. Phys.* 115:133–48
Sterling AC. 1994. See Enome & Hirayama 1994, pp. 131–33
Strong KT, Harvey K, Hirayama T, Nitta N, Shimizu T, Tsuneta S. 1992. *Publ. Astron. Soc. Jpn.* 44:L161–66
Struminsky A, Matsuoka M, Takahashi K. 1994a. *Ap. J.* 429:400–5
Struminsky A, Matsuoka M, Takahashi K. 1994b. See Enome & Hirayama, pp. 405–8
Sturrock P. 1980. In *Solar Flares: A Monograph from the Solar Skylab Workshop II,* ed. PA Sturrock, pp. 411–49. Boulder: Colo. Assoc. Univ. Press. 513 pp.
Sturrock PA. 1966. *Nature* 211:695–7
Svestka Z. 1976. *Solar Flares.* Dordrecht: Reidel. 399 pp.
Takakura T, Inda M, Makishima K, Kosugi T, Sakao T, et al. 1993. *Publ. Astron. Soc. Jpn.* 45:737–53
Terekhov OV, Syunyaev RA, Kuznetsov AV, Barat C, Talon R, et al. 1993. *Astron. Lett.* 19(2):65–68
Thompson DJ, Bertsch DL, Fichtel CE, Hartman RC, Hofstadter R, et al. 1993. *Ap. J. Suppl.* 86:629–56
Trottet G, Chupp EL, Marschhäuser H, Pick M, Soru-Escaut I, et al. 1994. *Astron. Astrophys.* 288:647–55
Tsuneta S. 1985. *Ap. J.* 290:353–58
Tsuneta S, Hara H, Shimizu T, Acton LW, Strong KT, et al. 1992. *Publ. Astron. Soc. Jpn.* 44:L63–69
Uchida Y, McAllister A, Khan J, Sakurai T, Jockers K. 1994. *Proc. Int. Symp. on the Yohkoh Scientific Results, Sagamibara, Kanagawa,* ed. Y Uchida, T Watanabe, K Shibata, HS Hudson, pp. 161–64. Tokyo: Universal Acad. Press
Van Driel-Gesztelyi L, Hudson HS, Anwar B, Hiei E. 1994. *Sol. Phys.* 152:145–51
Vestrand WT, Forrest DJ. 1993. *Ap. J. Lett.* 409:L69–72
Vestrand WT, Forrest DJ, Chupp EL, Rieger E, Share GH. 1987. *Ap. J.* 322:1010–27
Vilmer N. 1994. *Ap. J. Suppl.* 90:611–21
Vlahos L. 1994. *Space Sci. Rev.* 68:39–50
Wang H, Ewell MW Jr, Zirin H, Ai G. 1994. *Ap. J.* 424:436–43
White SM. 1994. See Ryan & Vestrand 1994, pp. 199–204
White SM, Kundu MR, Bastian TS, Gary DE, Hurford GJ, et al. 1992. *Ap. J.* 384:656–64
Wild JP, Smerd SF, Weiss AA. 1963. *Annu. Rev. Astron. Astrophys.* 1:291–366
Woodgate BE, Robinson RD, Carpenter KG, Maran SP, Shore SN. 1992. *Ap. J. Lett.* 397:L95–98
Wülser J-P, Canfield RC, Acton LW, Culhane JL, Phillips A, et al. 1994. *Ap. J.* 424:459–65
Yoshimori M, Takai Y, Morimoto K, Suga K, Ohki K. 1992. *Publ. Astron. Soc. Jpn.* 44:L107–10